



Review

A Comprehensive Review of Genetically Engineered Mouse Models for Prader-Willi Syndrome Research

Delf-Magnus Kummerfeld ¹, Carsten A. Raabe ^{2,3}, Juergen Brosius ^{3,4}, Dingding Mo ⁵, Boris V. Skryabin ^{1,*} and Timofey S. Rozhdestvensky ^{1,*}

- ¹ Medical Faculty, Core Facility Transgenic Animal and Genetic Engineering Models (TRAM), University of Muenster, Von-Esmarch-Str. 56, D-48149 Muenster, Germany; delf-magnus.kummerfeld@ukmuenster.de
- ² Research Group Regulatory Mechanisms of Inflammation, Institute of Medical Biochemistry (ZMBE), University of Muenster, Von-Esmarch-Str. 56, D-48149 Muenster, Germany; raabec@uni-muenster.de
- ³ Institute of Experimental Pathology (ZMBE), University of Muenster, Von-Esmarch-Str. 56, D-48149 Muenster, Germany; RNA.world@uni-muenster.de
- ⁴ Institutes for Systems Genetics, West China Hospital, Sichuan University, Chengdu 610041, China
- ⁵ School of Chemical Biology and Biotechnology, Peking University Shenzhen Graduate School, Shenzhen 518055, China; modingding@163.com
- * Correspondence: skryabi@uni-muenster.de (B.V.S.); rozhdest@uni-muenster.de (T.S.R.)

Abstract: Prader-Willi syndrome (PWS) is a neurogenetic multifactorial disorder caused by the deletion or inactivation of paternally imprinted genes on human chromosome 15q11-q13. The affected homologous locus is on mouse chromosome 7C. The positional conservation and organization of genes including the imprinting pattern between mice and men implies similar physiological functions of this locus. Therefore, considerable efforts to recreate the pathogenesis of PWS have been accomplished in mouse models. We provide a summary of different mouse models that were generated for the analysis of PWS and discuss their impact on our current understanding of corresponding genes, their putative functions and the pathogenesis of PWS. Murine models of PWS unveiled the contribution of each affected gene to this multi-faceted disease, and also enabled the establishment of the minimal critical genomic region (*PWS_{cr}*) responsible for core symptoms, highlighting the importance of non-protein coding genes in the PWS locus. Although the underlying disease-causing mechanisms of PWS remain widely unresolved and existing mouse models do not fully capture the entire spectrum of the human PWS disorder, continuous improvements of genetically engineered mouse models have proven to be very powerful and valuable tools in PWS research.

Keywords: Prader-Willi syndrome (PWS); Snord116; mouse models; Magel2; PWS imprinting center (IC); non-coding RNAs



Citation: Kummerfeld, D.-M.; Raabe, C.A.; Brosius, J.; Mo, D.; Skryabin, B.V.; Rozhdestvensky, T.S. A Comprehensive Review of Genetically Engineered Mouse Models for Prader-Willi Syndrome Research. *Int. J. Mol. Sci.* **2021**, *22*, 3613. <https://doi.org/10.3390/ijms22073613>

Academic Editor: Jens Høiriis Nielsen

Received: 28 February 2021

Accepted: 28 March 2021

Published: 31 March 2021

Publisher's Note: MDPI stays neutral with regard to jurisdictional claims in published maps and institutional affiliations.



Copyright: © 2021 by the authors. Licensee MDPI, Basel, Switzerland. This article is an open access article distributed under the terms and conditions of the Creative Commons Attribution (CC BY) license (<https://creativecommons.org/licenses/by/4.0/>).

1. Prader-Willi Syndrome

Prader-Willi syndrome (PWS; MIM#176270, <https://www.omim.org/entry/176270>, accessed on 20 March 2021) is a rare, neurodevelopmental, multifactorial genetic disorder resulting from the deletion or silencing of imprinted genes on paternally inherited chromosome 15q11–q13 [1–3]. PWS is chiefly caused by a large *de novo* deletion on chromosome 15q11–q13 (~60–70% of cases) (Figure 1A,B(1.,2.)). Approximately 25–35% of cases are caused by maternal uniparental disomy (i.e., two copies of maternal chromosomes UPD15) [4,5]. Less than 5% of PWS patients display defects of the genomic imprinting center (IC) and cases with sporadic chromosomal rearrangements or translocations were rarely identified [5–7].

The complex symptomology of PWS is divided into two main and phenotypically opposing stages. The onset of the first stage takes place during the last trimester of pregnancy and proceeds into infancy until around the ninth month. It is characterized by decreased

movement and reduced fetal growth in utero, neonatal hypotonia, feeding difficulties and postnatal failure to thrive. This is followed by a transitional phase lasting about five to eight years with comparatively normal weight gain. The second and final stage begins around age eight and extends into adulthood [4,8]. This stage is dominated by hyperphagia and a general lack of satiety; if uncontrolled, significant weight gain ensues transitioning into morbid obesity accompanied by all associated comorbidity risks. PWS patients suffer from general and continued developmental delay, short stature, small extremities and decreased muscle mass. They are frequently affected by respiratory malfunction symptoms, sleep disorders, hypogonadism, mild mental deficiency, and disruptions of their endocrine axis. Individuals display behavioral abnormalities including temper tantrums, obsessive compulsion and skin picking [4,9–11]. PWS is a complex disease, and symptoms vary considerably between patients, depending on the size of the chromosomal deletion [2,12,13]. Its prevalence ranges from 1 in 15,000–30,000 births with no observed difference between sexes or ethnicities [1,14–17]. PWS has a severe impact on the health and life expectancy of affected individuals, leading to a mortality of about 3% per year (approximately three times higher than that of the normal population). Main causes of death are related to respiratory failure, cardiovascular arrest, gastrointestinal blockage as well as infections, pulmonary embolisms and choking [18–20]. Therapeutic interventions focus mainly on infant feeding assistance, growth hormone replacement and endocrine dysfunction compensation as well as the treatment of various comorbidities arising from obesity [21–24]. After more than six decades of research since PWS was first described in 1956, a causative therapy does not exist (MIM#176270, <https://www.omim.org/entry/176270>, accessed on 20 March 2021).

2. The Prader-Willi Syndrome Locus in Mice and Men

Genomic imprinting is an epigenetic process, which via DNA and histone methylation restricts the expression of affected genes in a parent-of-origin specific manner. From the perspective of genome encoded function, the corresponding genes represent a haploid genotype. Loss of the remaining active allele results in expression defects. Historically, PWS was the first identified and characterized disease caused by an imprinting defect and/or uniparental maternal disomy [25,26]. The PWS genomic region harbors protein coding and non-protein coding genes as well as several regulatory elements that modulate imprinting and gene expression (Figure 1). The genomic structure of the PWS locus is highly conserved in mammals, with the murine PWS region on chromosome 7C being almost identical to that of human on chromosome 15. With the exception of the protein-coding gene *Frat3*, which is present only in mice, and reversely for rodents, no homolog to human *NPAP1* (*C15ORF2*) and non-protein coding *SNORD108* or *SNORD109A-B* genes could be identified (Figure 1) [27–32]. The conservation of gene organization and imprinting pattern between mice and humans implies similar physiological functions. Therefore, genetically modified mice can represent appropriate models and tools for the investigation of this disease [33].

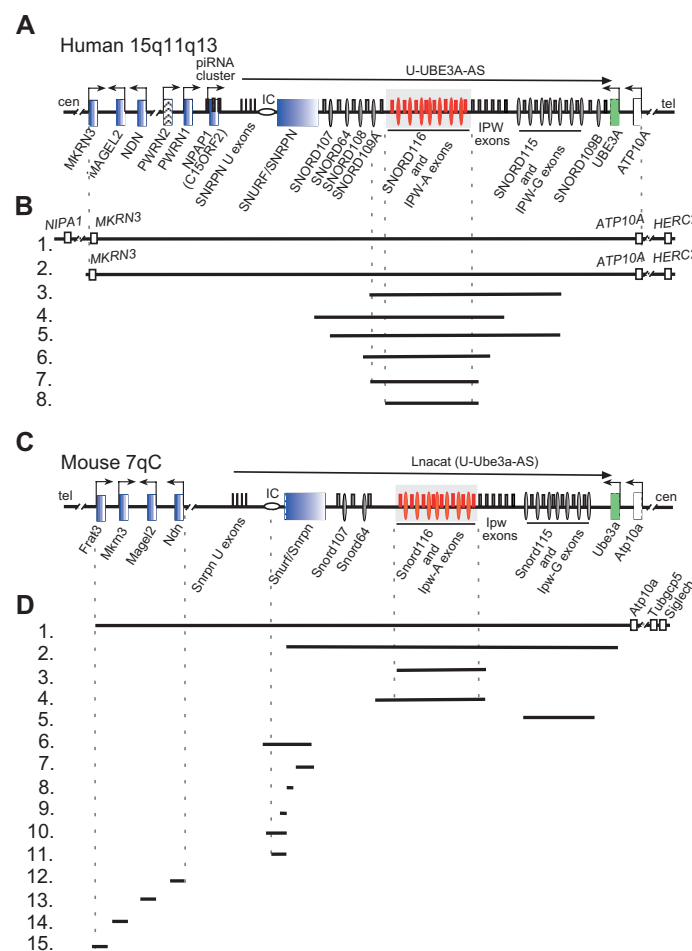


Figure 1. Organization of human and mouse PWS loci, deletions in human and PWS mouse models are indicated. **(A)** Schematic representation of the human PWS locus on chromosome 15q11-q13. Blue rectangles denote paternally imprinted protein coding genes. Thin ovals show snoRNA gene locations; the imprinting center (IC) is denoted by a horizontal oval. Thin rectangles above the midline depict non-protein coding exons. SNORD116 and IPW-A exons are displayed in red and further highlighted by a grey rectangle. Arrows indicate promoters and the direction of transcription. The long arrow on top shows the putative U-UBE3A antisense transcript harboring the SNORD116 and SNORD115 clusters. Centromere and telomere regions are indicated as cen and tel. **(B)** Schematic representation of PWS chromosomal deletions. Lines 1 and 2 indicate the common 5–6 Mb PWS deletion [2]. Lines 3–8 represent the characterized PWS cases with microdeletion in the Snord116 array. Line 3.—[34], 4.—[35], 5.—[36], 6.—[37], 7.—[38], 8.—[39] **(C)** Schematic representation of the mouse PWS-locus on chromosome 7qC (symbols as above). **(D)** Schematic representation of available mouse models in PWS research. (1.) The largest chromosomal deletion that eliminates the PWS/AS region and a large portion of non-imprinted genes [40]. (2.) Deletion of the mouse PWS-locus span from the *Snurf/Snrpn* to *Ube3a* genes [41]. (3.) Deletion of the PWS critical region (~300 kb) (*PWSscr*) comprising of *Snord116* and *IPW-A* gene arrays [42]. (4.) The *Snord116del* mouse model eliminating a larger ~350 kb *PWSscr* genomic region [43]. Note, that the genomic assembly of *PWSscr* is not completed, a gap of ~50 kb inside the *Snord116* cluster might increase the snoRNA gene copy number and overall size of deletion (UCSC, GRCm39/mm39 chr7:59457067- 59507068). (5.) Deletion of the *Snord115* gene cluster [44] (6.–11.) Deletions within the *Snurf/Snrpn* and PWS IC center (Details in Figure 2). (6.) 35 kb deletion of IC center and *Snurf/Snrpn* exons 1–6 [45]. (7.) Deletion of *Snurf/Snrpn* exon 6 including parts of exons 5 and 7 [45]. (8.) Deletion of *Snurf/Snrpn* exon 2 [41]. (9.–11.) Elimination of *Snurf/Snrpn* exon 1 and upstream genomic region: 0.9 kb (8), 4.8 kb (9) and 6 kb (10) deletions, respectively [46,47]. (12.–15.) Deletion of protein coding genes within the PWS-locus: (12.) *Ndn* [48–51]; (13.) *Magel2* [52,53]; (14.) *Mkrn3* [54]; (15.) *Frat3* [30].

3. PWS Uniparental Disomy (UPD) Murine Models

Maternal uniparental disomy (UPD) of chromosome 15 is the second most common genetic abnormality associated with PWS and is responsible for approximately 35% of cases [5]. Mice with maternal uniparental disomy of the central region on chromosome 7 constituted the first PWS genetic model [55]. It was generated by crossbreeding animals with X-autosomal translocations of the respective region [55]. Newborn pups exhibited weak suckling activity, failure to thrive and ultimately died within two to eight days following birth. No expression of *Snrpn/Snurfl* gene was detectable in the brain of mutant pups, suggesting an imprinting defect [55].

This very first model underlined the importance of the paternal allele in the pathogenesis of PWS in mice and defined future efforts to identify the PWS critical genomic region (Table 1).

Table 1. PWS mouse models and involved genes.

Gene(s) of Interest.	Name, Aliases	Phenotype	References
<i>all</i> (UPD Chr 7)	T(7;18)50H/+ (JAX001816, https://www.jax.org/strain/001816 , accessed on 20 March 2021)	postnatal lethality (100%) growth retardation	[55] *
<i>all</i> (6.8 Mb deletion)	<i>PWS</i> ^{ΔLMP2A} <i>Tg</i> ^{PWS/AS(del)} Del(7Herc2-Mkrn3)13FRdni/+	fetal growth retardation postnatal growth retardation neonatal lethality (100%) reduced movement irregular respiratory rate hypoglycemia pancreatic apoptosis insulin ↓, glucagon ↓ corticosterone ↑, ghrelin ↑	[40] * [56–58]
<i>Frat3</i>	<i>Frat3</i> ^{lacZ} <i>Peg12</i> ^{tm1Brn}	none	[30] *
<i>Mkrn3</i>	<i>Mkrn3</i> ^{m+/p-}	lower weight from P45 earlier onset of puberty GnRH1 ↑	[54] *
<i>Magel2</i>	<i>Magel2</i> ^{m+/p-} <i>Magel2</i> KO C57BL/6- <i>Magel2</i> ^{tm1Stw} /J (JAX009062, https://www.jax.org/strain/009062 , accessed on 20 March 2021)	<i>116HG</i> expression ↓ postnatal lethality (~10%) reduced weight until P28 body fat ↑ lean mass ↓ bone mineral density ↓ impaired glucose homeostasis impaired cholesterol homeostasis insulin resistance leptin resistance dopamine ↓, serotonin ↓ adiponectin ↑ corticosterones ↑ oxytocin ↓ different feeding behavior less active anxiety impaired social behavior delayed onset of puberty progressive infertility	[53] * [59–72]

Table 1. Cont.

Gene(s) of Interest.	Name, Aliases	Phenotype	References
<i>Magel2</i>	<i>Magel2</i> ^{m+/p-} <i>Magel2</i> ^{tm1.1Mus}	postnatal lethality (~50%) weak suckling oxytocin ↓, orexin-A ↓ abnormal social behavior impaired learning ability	[52] * [73]
<i>Magel2</i> (overexpression of truncated protein)	<i>CAG-trMagel2</i>	neonatal lethality (100%) small body size, poor suckling	[74] *
<i>Necdin</i>	<i>Ndn</i> ^{m+/p-} <i>Ndn</i> ^{tm1Alb}	none	[51] *
<i>Necdin</i>	<i>Ndn</i> ^{tm2Stw} B6.129S1(Cg)- <i>Ndn</i> ^{tm2Stw/J} (JAX009089, https://www.jax.org/strain/009089 , accessed on 20 March 2021)	postnatal lethality (80–95% C57BL/6 and 25% FVB) respiratory distress	[48] * [75,76]
<i>Necdin</i>	<i>Ndn</i> ^{m+/p-} B6.129S2- <i>Ndn</i> ^{tm1.1Mus}	postnatal lethality (21–31%) respiratory distress oxytocin ↓ serotonin ↓	[50] * [77,78]
<i>Necdin</i>	<i>Ndn</i> ^{m+/p-} <i>Ndn</i> ^{tm1Ky}	respiratory abnormalities DRG neuron apoptosis ↑ pain sensitivity ↓ noradrenergic excitability ↓	[49] * [79]
<i>Necdin</i>	<i>Ndn</i> ^{m+/p-} <i>Necdin</i> KO <i>necdin</i> ^{m+/p-}	unstable circadian rhythm	[80] *
<i>Snurf/Snrpn</i> <i>Snord116</i> IPW <i>Snord115</i> <i>Ube3a</i>	<i>Snrpn-Ube3a</i> deletion Del(7Ube3a-Snrpn)1Alb	neonatal lethality (80%) growth retardation hypotonia	[41] *
<i>all</i> (IC deletion)	<i>PWS-IC</i> ^{Δ35kb} <i>Snrpn</i> ^{tm2Cbr} <i>ΔPWS-IC</i> <i>PWS-IC</i> ^{del} <i>PWS-IC</i> ^{del35kb} B6.129-Snrpn ^{tm2Cbr/J} (JAX012443, https://www.jax.org/strain/012443 , accessed on 20 March 2021)	neonatal lethality (40–90% depending on background) growth retardation hypotonia decreased locomotive ability abnormal behavior ghrelin ↑ increased food consumption food-seeking behavior ↑	[45] * [81–86]
<i>all</i> (IC deletion)	<i>PWS-IC</i> ^{m+/p del4.8kb} <i>PWS-IC</i> ^{Δ4.8} <i>Snrpn</i> ^{tm2Alb}	neonatal lethality (40%) growth retardation	[46] *
<i>all</i> , except <i>Snrpn</i> , <i>Snord64</i> , 116, 115 (IC deletion)	<i>PWS-IC</i> ^{Hs} <i>Snrpn</i> ^{tm1Kaj}	neonatal lethality (47% C57BL/6J and 16% 129S1/Sv) growth retardation feeding difficulties	[87] *
<i>all</i> (IC deletion)	<i>PWS-IC</i> ^{m+/pΔ6kb} <i>PWS-IC</i> ^{Δ6kb} B6.129S1- <i>Snrpn</i> ^{tm2.1Kaj/J} (JAX018395, https://www.jax.org/strain/018395 , accessed on 20 March 2021)	neonatal lethality (100%) growth retardation feeding difficulties	[47] *

Table 1. Cont.

Gene(s) of Interest.	Name, Aliases	Phenotype	References
<i>Snord116</i> /IPW	<i>PWScr</i> ^{m+/p-} Del(7lpw-Snord116)1Jbro (distributed by TRAM Münster)	neonatal lethality (15%) growth retardation <i>pOx</i> ↑, <i>Peg3</i> ↑ decreased gray-matter volume altered sleep profile altered body temperature	[42] * [88,89]
<i>Snord116</i> /IPW	<i>Snord116del</i> <i>Snord116</i> ^{tm1Uta} <i>Snord116</i> ^{+/-P} B6(Cg)- <i>Snord116</i> ^{tm1.1Uta} /J (JAX008149, https://www.jax.org/strain/008149 , accessed on 20 March 2021)	growth retardation <i>Igf1</i> ↓ ghrelin ↓ impaired pancreatic development altered diurnal methylation increased anxiety altered respiratory exchange rate resistant to obesity	[43] * [90–94]
<i>Snord116</i> /IPW (homozygous)	<i>Snord116</i> ^{m-/p-} <i>Snord116</i> ^{-/-}	growth retardation fat mass ↓ increased food consumption altered diurnal activity profile resistant to obesity altered hypothalamic signaling	[95] *
<i>Snord116</i> /IPW (only <i>Npy</i> ⁺ Neurons)	<i>Snord116</i> ^{lox/lox} /NPY ^{cre/+} (JAX008118, https://www.jax.org/strain/008118 , accessed on 20 March 2021)	growth retardation fat mass ↓ increased food consumption altered diurnal activity profile altered hypothalamic signaling	[95] *
<i>Snord116</i> /IPW (adult-onset)	<i>Snord116</i> deletion	reduced food consumption insulin resistance	[96] *
<i>Snord116</i> /IPW (adult-onset)	AAV- <i>Snord116del</i> ^{m+/p-} <i>Snord116</i> ^{fl} AAV-Cre	increased food consumption bodyweight ↑ bodyfat percentage ↑	[91] *
<i>Snord115</i>	<i>Snord115</i> -deficient	brown adipose tissue ↑ modest alterations in 5-Htr2cr mRNA A-to-I editing	[44] *
<i>Snord116</i> (single copy transgene)		no effect on phenotype	[43] *
<i>Snord116</i> (transgene 2 mouse, 1 rat copies)	<i>PWScr</i> ^{m+/p-} -Tg <i>Snord116</i>	no effect on phenotype	[97] *
<i>Snord116</i> (transgene 27 copies)		no effect on phenotype	[98] *
<i>all</i> (biallelic IC deletion)	<i>PWS-IC</i> ^{mΔ4.8kB/pΔ4.8kB} <i>PWS-IC</i> ^{mΔ4.8kB/pΔS-U}	rescue of postnatal lethality rescue of growth retardation	[99]
<i>Snord116</i> /IPW (maternal IC deletion)	<i>PWScr</i> ^{m5'LoxP/p-} (distributed by TRAM Münster)	Rescue of growth retardation in adult mice alterations in 5-Htr2cr mRNA A-to-I editing in the choroid plexus.	[97] *
<i>Snord116</i> (AAV-mediated)	<i>Snord116del</i> ^{m-/p-} AAV- <i>Snord116</i>	energy expenditure ↑ rate of weight gain ↓	[100] *

Original publications are marked by *, up- and downregulation of physiological parameters is represented by arrows (↑ and ↓).

4. PWS Large Chromosomal Deletion Models

In humans, large deletions on paternal chromosome 15q11.2-q13 were detected in more than 60% of diagnosed PWS cases—indicating that this is the most common underlying cause of the disease [5].

A mouse model with a deletion of the entire *PWS* region was generated more than two decades ago by microinjecting a fragment of an Epstein-Barr Virus Latent Membrane Protein 2A (*LMP2A*) vector into mouse zygotes (B6×SJL) F1 [40]. The resulting transgene contained a 6.8 Mb long array of ~80 repeated *LMP2A* copies that replaced all imprinted genes in the PWS region (Figure 1C,D; Table 1) [56]. For over four generations, the resulting transgenic *PWS*^{ΔLMP2A} (*TgPWS*) mice were bred with C57Bl/6 and subsequently with CD1 wild-type mice for the same number of generations. Finally, one stable viable transgenic mouse line derived from a single founder was established.

For *TgPWS* mice with a maternally inherited modified chromosome, no phenotypic abnormalities were observed. This is in stark contrast to paternal inheritance of the modified locus, which led to failure to thrive with fetal and neonatal growth retardation, reduced movement and irregular respiratory rates. Expression of all imprinted genes from the PWS locus was abolished and mice eventually died within one week of birth due to severe hypoglycaemia [57]. Deregulation of the hepatic Igf (Insulin growth factor) axis and increased concentrations of corticosterone and ghrelin were reported for mutant mice. *TgPWS* mice also displayed elevated levels of pancreatic apoptosis; this, in turn led to reduced α - and β -cell masses and lowered levels of pancreatic islet hormones (i.e., insulin and glucagon) [58]. The comprehensive analysis of this mouse model with a large chromosomal deletion in the PWS-locus convincingly demonstrated that the elimination of imprinted genes causes a large spectrum of PWS-related abnormalities associated within the early postnatal period.

In contrast to human, the elimination of all genes within the PWS-locus resulted in early postnatal lethality in mice, which makes it almost impossible to use this model in the detailed investigations of the complete spectrum of PWS pathogenesis. Undoubtedly, however, this mouse model confirmed that these human and mouse loci are functionally similar, which justified the utilization of genetically engineered mouse models to examine PWS-related genes in order to advance our understanding of the human syndrome.

5. *Frat3*

The murine *Peg12/Frat3* gene (paternally expressed gene 12/frequently rearranged in advanced T-cell lymphomas 3) has no orthologue in the human PWS locus. The single CDS (Coding Sequence) exon encodes a 283 amino acid long protein, which is implicated in canonical Wnt signaling via binding to GSK-3 β [101,102]. A knockout mouse model was generated in the 129/Ola background; most of the *Frat3* coding sequence, i.e., including the start codon, was replaced with a *lacZ*-reporter gene cassette, thereby leaving its original promoter intact. Homozygous *Frat3*^{lacZ} mice lacked any obvious phenotype (Table 1) [30]. Moreover, molecular analysis of *Frat*-deficient mice revealed that it is not an essential component of the canonical Wnt pathway in mammals, and *Frat3* is not involved in the PWS phenotype in mouse models [30].

6. *Mkrn3*

Intronless *Mkrn3* (makorin RING-finger protein 3 [formally *Zfp127*]) encodes a putative E3 ubiquitin ligase of 544 amino acids (Figure 1); it inhibits the hypothalamic–pituitary–gonadal axis, thereby modulating the onset of puberty in mammals [103].

Mkrn3 knockout mice were generated on the C57BL/6 wild-type background via the introduction of an engineered 2 bp frameshift deletion at position 275–276 of the ORF (Open Reading Frame) in the single CDS exon of the gene (Table 1) [54]. Mating of *Mkrn3*^{m+/p-} males with WT (wild-type) females yielded offspring in the expected Mendelian ratio. Compared to their respective WT littermates of the same sex and age, *Mkrn3*^{m+/p-} male mice were noticeable lighter between postnatal day P15 to P60. The corresponding weight

gain for female *Mkfn3*^{m+/p-} mice proceeded biphasically; KO (knockout) mice were heavier between day P15 to P40, but gained less weight compared to age-matched controls from day P45 to P60. Another effect of the *Mkfn3* knockout was the earlier onset of puberty in both sexes, induced by an increased production of hypothalamic GnRH1 (gonadotropin-releasing hormone).

MKRN3 is an unlikely contributor to the key symptoms of PWS in humans [104]. However, these findings advanced our understanding of general regulatory mechanisms of the pubertal process and putative molecular defects causing PWS-related hypogonadism. Moreover, the genetically engineered *Mkfn3*^{m+/p-} mouse model served as a useful tool to investigate the molecular mechanism underlying human central precocious puberty (CPP) syndrome.

7. Magel2

MAGEL2 (Melanoma Antigen-subfamily like 2) is another paternally imprinted intronless gene, within the PWS locus (Figure 1) [64,72,105]. The human gene encodes a protein of 529-amino acids (525 amino acids in mouse) that displays about 51% sequence similarity to *NECDIN*, and functions as an E3 ubiquitin ligase enhancer involved in retromer endosomal protein trafficking [106–108]. *MAGEL2* is particularly interesting, as patients with inactivated mutations of this gene develop the Schaaf-Yang syndrome (SYS; MIM#615547, <https://www.omim.org/entry/615547>, accessed on 20 March 2021). SYS shares many symptoms with PWS, including neonatal hypotonia, feeding difficulties, developmental delay, hypogonadism, intellectual disability, and a prevalence to autism-related disorder [109–111].

For the *in vivo* investigation of *MAGEL2* functions, C57Bl6-derived *Magel2*^{m+/p-} mice were generated by replacing the C-terminus of the open reading frame with a lacZ reporter (Table 1) [53]. Although the promoter region remained intact, these mice entirely lacked *Magel2*-LacZ fusion protein expression [53,59]. Subsequent analysis revealed that in addition to *Magel2*-LacZ, the expression of the *Ipw-A* non-protein coding transcript was significantly reduced. The *Magel2*^{m+/p-} neonates displayed a postnatal lethality of ~10%, failure to thrive and growth retardation, resulting in a slight decrease in body weight until weaning (~P28). After weaning, mutant mice equaled the body weight of their WT littermates; however, KO mice were characterized by higher body fat percentage as well as decreased lean mass and muscle fibers. In addition, the bone mineral density was decreased [53,59,61,63,64,67]. When *Magel2* KO mice were fed a standard diet for 12–14 weeks, a slight increase in body weight—compared to WT littermates—was observed [59,69]. Glucose and cholesterol homeostasis was impaired in *Magel2* KO mice. In addition, signs of insulin and leptin resistance, defective responses to ghrelin stimulation, higher serum adiponectin concentrations, elevated corticosterones, a malfunctioning growth hormone axis and compromised melanocortin signaling were identified [59,62,64–66,112]. Changes in oleoylethanolamide signaling were also reported [69]. Concentrations of several neurotransmitters were lower in *Magel2*-null mouse brains, including those of dopamine and serotonin [60,70]. In addition, the lack of *Magel2* in KO mice was accompanied by reduced levels of several neuropeptides, i.e., oxytocin and orexins. Furthermore, the expression of regulatory proteins that participate in processing and exocytosis of neuropeptides via secretory granules was compromised [53,71,72]. *Magel2* null mice also revealed higher levels of mTOR and its downstream signaling targets in the hypothalamus [68]. The mutant mice displayed different feeding behavior, most notably an increased portion size and time per meal after a 24 h fast [69]. *Magel2*^{m+/p-} mice were on average less active, both in familiar and novel environments [53,61]. They exhibited increased anxiety and impaired social behavior [60,113]. Absence of *Magel2* expression reduced the reproductive fitness in both sexes, results in delayed onset of puberty and irregular estrous cycles in females and decreased olfactory preference for aesthetic female odor as well as significantly reduced levels of serum testosterone in males [60].

An independent KO model for *Magel2* was generated on a 129Sv/Pas genetic background. The entire gene promoter and approximately 75% of the CDS were deleted (Table 1). The resulting mice were subsequently backcrossed to the C57Bl6/J background [52]. *Magel2*^{m+/p-} neonates were not hypotonic, but sustained significantly (~50%) increased lethality, caused by weak or even absent suckling activity. Lack of *Magel2* expression also impaired the production, particularly the processing from precursor to active peptide of hypothalamic neuropeptides, such as oxytocin and orexin-A. *Magel2* mutants also exhibited deficiencies in social behavior and learning abilities [73]. The suckling initiation deficit phenotype as well as the development of behavioral abnormalities could be resolved by the injection of oxytocin in the first postnatal week [52,73].

More than half of SYS patients express a truncated version of *MAGEL2*, which is the result of mutation or deletion within the so-called proline-rich region upstream of the C-terminus [109]. Two additional mouse models were generated to analyze the functional impact of these variants. One represented a similarly truncated version of *Magel2* (*trMagel2*) as detected in SYS patients, and a second overexpressed the transgenic *Magel2* (CAG-*trMagel2*) N-terminal domain (amino acid residues 1–437) under the control of the CAG promoter (Table 1) [74]. Overexpression of the *Magel2* truncated protein was highly toxic, as all CAG-*trMagel2* positive pups died between birth and postnatal day 13. Heterozygous mice carrying the truncated *trMagel2* on either the paternal *Magel2*^{m+/p-tr} or maternal *Magel2*^{m-tr/p+} allele had no obvious phenotype. The neonatal *Magel2*^{m+/p-tr} pups were lighter than their wild-type littermates but gained weight faster until there was no detectable difference at the age of eight weeks.

Mice lacking *Magel2* recapitulate a basic aspect of PWS and SYS stage I. However, none of the models developed the more severe symptoms of later stages of PWS, severe obesity combined with hyperphagia. Nevertheless, understanding the physiological function of *Magel2*, particularly its role in the proteolytic processing pathways of several hormones, implies an important contribution to many symptoms associated with PWS and SYS.

8. Necdin

The intronless *Necdin* (*NDN*) gene encodes a 321 amino acids long protein which is a member of the MAGE family and implicated in cell survival, maintenance of circadian rhythm [80], neuron migration and growth [114,115]. Neurological symptoms in PWS patients suggested a functional role of *NDN* in the pathophysiology of the disease [116]. To analyze *Ndn* functions in vivo, several knockout mouse models were generated. The first model was engineered in the 129SV mouse background (Table 1). The entire CDS and promoter region of *Ndn* was replaced by a β -Galactosidase reporter [51]. The resulting mice were null for *Ndn* expression. Both homo- and heterozygous mutants were viable, had normal fertility, showed the same body weight development as WT mice and did not develop obesity until 10 months of age.

In-frame fusion of the first 31 *Ndn* codons with a *lacZ* reporter and replacement of the downstream CDS with the cassette was used to generate a second KO model in 129Sv derived ES (Embryonic stem) cells (Table 1). The KO strategy left the endogenous promoter intact; the resulting chimeric males were crossed with C57BL/6 WT females [48]. Depending on the genetic background of the female, the resulting heterozygous offspring displayed varying degrees of postnatal lethality due to respiratory problems from 80–95% for C57BL/6 and 25% for FVB to WT levels for (C57BL/6 \times C3H)F1 hybrids. In most cases, the lethality was higher in male than female offspring. Respiratory distress originated from abnormalities in serotonergic modulation of the respiratory rhythm generating neurons, which are particularly sensitive to loss of *Ndn* expression [75,76]. The surviving mice were not associated with any detectable phenotype, did not develop obesity until 10 months of age and were fertile.

The third *Ndn* KO model was generated by replacing the promoter and two-thirds of the N-terminal *Ndn* coding sequence with the *Neo* cassette flanked by *LoxP* sites, which was subsequently removed by crossing with *Cre*-expressing C57Bl6/J females (Table 1) [50].

Heterozygous neonates displayed 21–31% lethality due to respiratory distress [50,67]. The surviving mice were fertile, exhibited normal weight development and did not become obese during an 18-month observational period. *Ndn*^{m+/p-} mice displayed a significant reduction in oxytocin-producing and luteinizing hormone-releasing hormone (LHRH)-producing neurons in hypothalamus. The *Ndn* null mutants had a normal circadian rhythm, normal motoric skills and showed no abnormalities in anxiety-related behavior, but were superior in spatial learning and memory tests. Notably, skin scraping was significantly increased in *Ndn*^{m+/p-} mice compared to the wild-type control. Homozygous *Ndn*^{m-/p-} offspring had an even higher postnatal lethality of 43% compared to heterozygotes, most likely due to respiratory deficiency [77]. Interestingly, low *Ndn* expression levels were detectable from the maternal allele in two *Ndn*^{m+/p-} mouse strains (C57Bl/6J and 129Sv/Pas). There was also a drastic (i.e., up to three orders of magnitude) inter-individual variability of *Ndn* expression between *Ndn*^{m+/p-} mice. Complete loss of *Ndn* expression in surviving homozygous mice altered the development and function of serotonergic neurons, resulting in central apnea and hypercapnia [78]. *Ndn*^{m+/p-} mice showed a significant, i.e., up to three-fold, upregulation of *Slc6a4* (serotonin transporter, solute carrier family 6 member 4) expression, which results in an increase of serotonin (re-)uptake and thereby decreased extracellular serotonin to insufficient levels, ultimately causing breathing deficits.

Another model was generated by conventional gene targeting, with a 1.5 kb *Pgk/NeoR* cassette inserted into the *Ndn* gene to disrupt its coding sequence (Table 1) [49]. The targeting vector was electroporated into TT2 ES cells. Positive clones were injected into ICR embryos and the resulting chimeras were backcrossed to ICR wild-type mice. The heterozygous *Ndn*^{m+/p-} mice did not reveal any increased postnatal lethality, were fertile and bred in the normal Mendelian ratio. Necdin deficiency triggered apoptosis in developing mouse dorsal root ganglia at E12.5 and led to a significant reduction in total neuron number at P0. The *Ndn*^{m+/p-} also had a significantly increased tolerance to pain compared to the wild-type control at the age of two and four weeks. Five-day-old *Ndn*^{m+/p-} neonates displayed some signs of hypotonia, although there were no significant differences by the age of two weeks [79]. The mutant also had an impaired ventilatory response to hypercapnia at postnatal days 4 and 8. The neurons of the noradrenergic system in the locus coeruleus of *Ndn*^{m+/p-} mice are characterized by decreased spontaneous activities and showed impaired excitability.

Recently, using CRISPR/Cas9-mediated genome engineering, a Necdin deficient mouse model harboring a 1349 bp deletion within the *Ndn* gene was generated on a C57BL/6 background (Table 1) [80]. Lack of necdin protein destabilized a key component of the circadian clock and resulted in alterations of clock gene expression compared to wild-type and an unstable circadian rhythm in *Ndn*^{m+/p-} mice.

The *Ndn* mouse models successfully reproduced both the respiratory and sleep disorder related phenotype of PWS; therefore, they are suitable for the development of novel therapeutic approaches, as respiratory failure is the most common cause of death in infants and children diagnosed with PWS [18]. As previously noted [117], it is remarkable that the majority of protein coding genes in this locus were generated via retrotransposition, emphasizing once more the significance of this mechanism for the evolution of genes and entire gene loci [118].

9. Snurf/Snrpn

The *SNURF/SNRPN* (Small Nuclear Ribonucleoprotein Polypeptide N) gene encodes two different proteins from a bicistronic transcript spanning 10 exons and is highly conserved between humans and mice [119]. CDS exons 1–3 encode for the 71 amino acids protein Snurf (SNRPN upstream open reading frame), while CDS exons 4–10 encode for a 240 amino acids component of the SmN complex (small nuclear ribonucleoprotein complex) [120]. The *SNURF/SNRPN* bicistronic transcript is highly expressed in the brain and heart in both humans and mice. *SNURF* localizes to the nucleus but its function is still unknown. SmN plays a role in pre-mRNA processing and possibly alternative

splicing, regulating the development of the spine and cerebral cortex in mice [121–123]. For numerous patients diagnosed with PWS, deletions of the *SNURF/SNRPN* gene were detectable, suggesting that its product(s) might contribute to the pathology of the disease [124–126]. For the analysis of *Snurf/Snrpn* functions, seven different genetically modified mouse models were generated (Figure 2). Three of them contained small deletions of the *Snurf/Snrpn* protein coding region, eliminating CDS exon 2, exons 5–7 and exon 1, respectively (Figure 2B–D). A fourth model harbored a long deletion eliminating *Snurf/Snrpn* exon 2 up to the *Ube3a* gene region (Figure 2A) [41,45]. Regardless of the actual mouse genetic background, i.e., C57BL/6 or 129/SvEv–C57BL/6] hybrids, the offspring with paternally inherited *Snurf/Snrpn* small deletions (Figure 2B–D) were indistinguishable from wild-type littermates. They exhibited a normal imprinting pattern, were fertile and displayed no obvious phenotypic abnormalities [41,45]

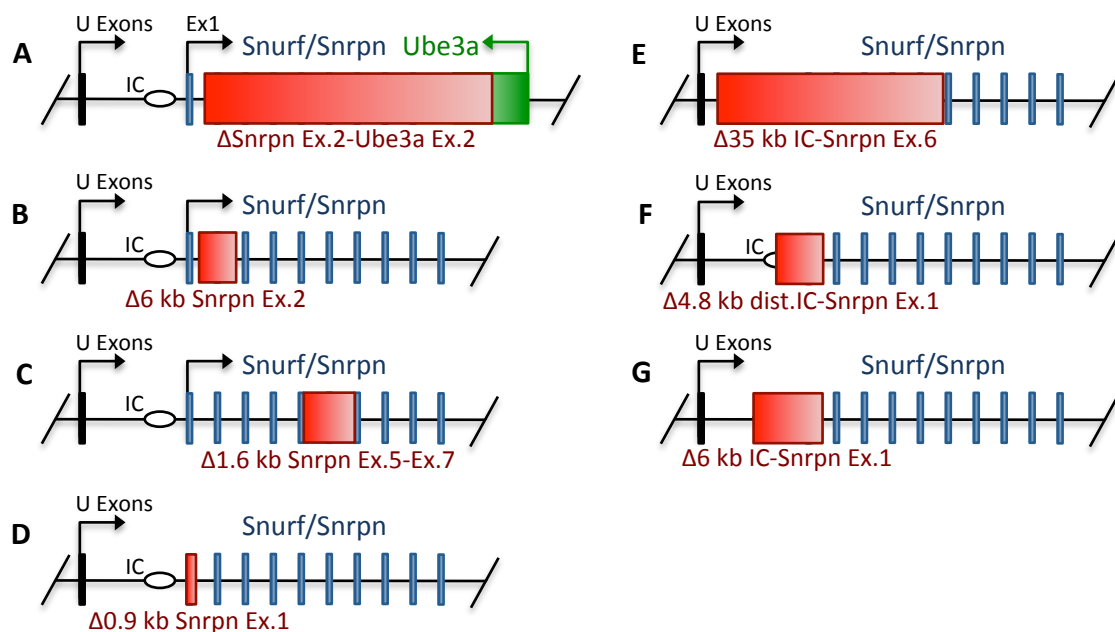


Figure 2. Schematic representation of genetically engineered mouse models harboring deletions within *Snurf/Snrpn* and PWS IC center (drawings are not to scale). Green and thin blue rectangles denote *Ube3a* and *Snurf/Snrpn* CDS exons, respectively. The red rectangles indicate generated genomic deletions. Thin black rectangles show location of U-exons; the imprinting center (IC) is denoted by a horizontal oval. (A). Large deletion of the genomic region between *Snurf/Snrpn* exon 2 and *Ube3a* exon 2. [41]. (B). Inactivation of the *Snurf* ORF by deleting the 6 kb region including *Snurf/Snrpn* exon 2 [41]. (C). Intragenic deletion of 1.6 kb within *Snurf/Snrpn* including exon 6 and parts of exons 5 and 7 disrupting the *Snrpn* ORF [45]. (D). Small 0.9 kb deletion of the major *Snurf/Snrpn* promoter together with first CDS exon [46]. (E). The PWS IC deletion, spanning 35 kb (originally described as 42 kb) including *Snurf/Snrpn* exons 1–6 [45]. (F). Deletion of 4.8 kb (later revealed to be 5.07 kb in size) genomic region, including *Snurf/Snrpn* exon 1 and the distal part of the PWS IC [46]. (G). The 6 kb deletion comprising PWS IC and *Snurf/Snrpn* exon 1 [47].

Different results were obtained in a mouse model with a deletion from *Snrpn* exon 2 to *Ube3a* (Figures 1D and 2A; Table 1) [41]. Mice homozygous for this long deletion did not survive past E20. Heterozygotes with the long deletion on the paternal allele were weak, hypotonic and had weak suckling activity. They were underweight at birth and showed severe growth retardation compared to WT littermates; only about 20% of the mutant pups survived until weaning. The surviving knockout mice were fertile, had about 2/3 of the bodyweight of age-matched WT animals, and did not develop obesity within a 14-month observational period [41]. These data raised doubts with regards to the functional significance of the *SNURF/SNRPN* gene as the primary cause of PWS and underlined the importance of the PWS critical region, which at the time, had not been identified.

10. PWS Imprinting Center

In the late nineties, a 35 kb deletion (originally reported as 42 kb) encompassing *SNURF/SNRPN* CDS exons 1–6 and its 16 kb upstream region was generated in C57BL/6 mice by replacing the corresponding sequence with a P_{gk}-Neo-polyA cassette (Figures 1D and 2E; Table 1) [45]. This deletion ($PWS-IC^{\Delta 35kb}$) resulted in a complete imprinting defect and thus abolished expression of all imprinted genes in the locus. $PWS-IC^{\Delta 35kb}$ neonates had decreased body weight and hypotonia at birth, resulting in poor suckling and low blood glucose levels. Ultimately, the offspring died within the first week due to feeding difficulties. However, this fully penetrant neonatal lethality was highly dependent on the genetic background. C57BL/6 males carrying the maternal $PWS-IC^{\Delta 35kb}$ allele produced viable offspring (survival rates between 10%–60%) with female mice of FVB/NJ, C3H/HeJ, 129S1/Sv and BALB/cJ genetic background, but not with C57BL/6J or DBA/2J animals [81]. Viable pups, especially after separation from WT siblings, grew into adulthood and were at all times smaller than WT controls. $PWS-IC^{\Delta 35kb}$ had normal fertility and did not develop obesity until the end of the 15-week observational period. The mouse background-dependent survival was putatively independent of residual expression of genes from the paternal chromosome or leakage from the maternal chromosome, since the detected expression levels did not correlate with survival rate [81]. The most likely explanation of the observed differences is strain specific gene-modifiers affecting survival [81]. $PWS-IC^{m+}/p\Delta 35kb$ mice generated by crossing $PWS-IC^{\Delta 35kb}$ C57BL/6J males to CD-1 females exhibited less locomotive activity and impaired attentional functions, but normal anxiety levels compared to WT [82]. Furthermore, $PWS-IC^{m+}/p\Delta 35kb$ mice showed increased impulsivity and locomotor activity when motivated by food reward [83]. There were no detectable differences in whole tissue monoamine levels or expression and splicing of 5Ht2cr (see below). The $PWS-IC^{m+}/p\Delta 35kb$ mice also underperformed in a stop-signal reaction time task compared to WT mice suggesting increased impulsivity. This effect could be ameliorated with the selective 5Ht2cr agonist WAY163909 [85]. Compared to the wild-type control, circulating ghrelin levels were elevated up to threefold in $PWS-IC^{m+}/p\Delta 35kb$ mice. Mutants were also characterized by significantly higher food consumption, both with ad libitum access and after an overnight fast [84]. In contrast to wild-type mice, $PWS-IC^{m+}/p\Delta 35kb$ mice reacted with apathy towards non-caloric sweetener and showed a preference for food of high caloric value. Interestingly, $PWS-IC^{m+}/p\Delta 35kb$ mice performed better in a maze-learning test than wild-type mice when combined with food reward. These findings might suggest increased motivation due to stronger food-seeking behavior [86].

To narrow down the critical size of the imprinting center, additional in vivo models were generated by targeting the DNA methylation region (DMR) located upstream of the *Snurf/Snrpn* CDS exons. Two models encompassing deletions of 0.9 kb and 4.8 kb were generated (Figure 2D,F; Table 1). The latter was later revealed to be 5.07 kb [47]; but, designated as $PWS-IC^{m+}/p\Delta 4.8kb$ model in the literature. Notably, the larger deletion eliminated almost the entire methylation region (~2.7 kb), leaving only a small part intact [46]. Heterozygous mice harboring the small deletion (0.9 kb) displayed a regular imprinting pattern, were phenotypically unremarkable, fertile and had no weight abnormalities compared to WT mice. The paternal inheritance of the 4.8 kb deletion, on the other hand, resulted in an approximate 40% postnatal lethality. The growth of surviving $PWS-IC^{m+}/p\Delta 4.8kb$ mice was retarded, amounting to a 30% decrease in size and bodyweight. However, the mutant mice harboring the paternal deletion were fertile. Notably, the 4.8 kb deletion resulted in a partial imprinting defect, therefore the $PWS-IC^{m+}/p\Delta 4.8kb$ mice displayed low expression levels of *PWS*-locus encoded genes.

To define the imprinting center of the mouse *PWS*-locus, a further model harboring a 6 kb deletion was generated, eliminating about 3.7 kb upstream from *Snurf/Snrpn* exon 1 (Figure 2G; Table 1) [47]. The 3' end of this 6 kb deletion was identical to that of the previously mentioned 4.8 kb deletion. The $PWS-IC^{m+}/p\Delta 6kb$ offspring containing the deletion on the paternally inherited chromosome were significantly smaller and weaker than their WT littermates. They often lacked milk spots and did not survive past postnatal

day 7, with most of the pups dying within 48 h after birth. *PWS-IC^{m+/pΔ6kb}* mice displayed no detectable expression of PWS genes from the paternal allele, indicating that functional elements enabling *PWS-IC* activity were present within the deleted interval [47].

For the investigation of the human PWS imprinting region, a knock-in transgenic mouse model was generated by replacing the mouse 6 kb *PWS-IC* with a 6.9 kb fragment of the entire human *PWS-IC* region (Table 1) [47,87]. Knock-in mice harboring human *PWS-IC^{Hs}* acquired maternal DNA methylation patterns. Paternal inheritance of the *PWS-IC^{Hs}* led to a neonatal lethality of 47% in the second generation with a C57BL/6J background and 16% postnatal lethality with a 129S1/Sv background. The *PWS-IC^{Hs}* mutant pups were significantly smaller, had difficulties feeding and displayed considerable growth retardation, which was accompanied by a 50% reduced bodyweight; the effect persisted into adulthood. Paternal inheritance of the *PWS-IC^{Hs}* resulted in almost complete absence of the *Ndn*, *Mkrn3*, *Mage12* and *Frat3* gene products, but expression of U-Ube3a-As derived non-protein coding RNAs, including Snord64, Snord116, Snord115 and Ube3a-As remained unaltered [87].

The data implied that the mechanism to acquire silencing is conserved between humans and mice, but the maintenance and regulation of the silenced state is different. This also might explain the differences in the regulation of tissue-specific expression of PWS encoded genes between both species [127]. In any event, the analysis conducted with these mouse models defined the PWS-locus imprinting center in mice and revealed that the imprinting effect is similar in mice and men.

11. Snord116 Gene Cluster

Imprinted SNORD small nucleolar RNAs (snoRNAs) within the PWS-locus were originally identified two decades ago [128]. Based on the presence of conserved C and D sequence motifs, these snoRNAs were assigned to the subclass of 2'-O-methylation guide C/D box snoRNAs. However, due to the apparent lack of any significant complementarities to classical snoRNA target molecules (rRNAs, snRNA) they are referred to as "orphan" snoRNAs [129]. The human PWS region harbors seven *SNORD* genes and families: *SNORD107*, *SNORD64*, *SNORD108*, *SNORD109A*, *SNORD116*, *SNORD115* and *SNORD109B*. The corresponding mouse locus contains the orthologous genes *Snord107*, *Snord64*, *Snord116* and *Snord115*. Most snoRNAs from the PWS-locus are processed from introns of a long primary non-protein coding U-UBE3A-AS transcript (U-Ube3a-AS in mouse) (Figure 1). Both the human and murine genes are paternally imprinted. In human, *SNORD116* and *SNORD115* genes represent tandemly repeated arrays comprised of 29 and 48 copies, respectively [129]. *SNORD116* copies are located within introns flanked by the repetitive *IPW-A* exons of the *U-UBE3A-AS* transcript (Figure 1A). *SNORD115* copies are embedded between repetitive *IPW-G* exons (Figure 1A). In mice, 66 copies of *Snord116* are distributed in the introns of 67 *Ipw-A* exons (Figure 1C). However, due to an assembly gap of approximately 50 kb inside the mouse *Snord116* region, the exact number of repeats is yet to be determined. Although *SNORD116* displays a high degree of sequence similarity between different mammalian species [130], conventional targets on rRNAs cannot be identified [128,129]. In rodents, expression of the PWS locus encoded snoRNAs is restricted to neurons, while in humans they are most abundant in brain but also expressed in other tissues [127].

11.1. The First Mouse Model Harboring the Deletion of the PWS Critical Region (*PWS^{Scr}m+/P-*)

Analysis of the aforementioned mouse models that abolished the expression of single or multiple genes predicted PWS critical region (*PWS^{Scr}*) within the *Snord116* gene cluster [131]. To investigate the putative contribution of *Snord116* to the PWS phenotype in vivo, two mouse models were generated. The first model harbored a ~300 kb genomic deletion (UCSC, GRCm39/mm39 chr7:59,277,590-59,580,881) of the *Snord116* and *Ipw-A* gene arrays and was designated as *PWS^{Scr}* deletion model (Figure 1 C,D; Table 1) [42]. *PWS^{Scr}m+/P-* pups displayed significant growth retardation starting from postnatal day 5

lasting into adulthood, i.e., up to one year of monitoring. Growth retardation was observed independent of the following genetic backgrounds: 129SV \times C57BL/6 (>85% C57BL/6 contribution), 129SV \times C57BL/6 \times FVB/N (~50% FVB/N contribution) as well as 129SV \times C57BL/6 \times BALB/c (~50% BALB/c contribution). A slight increase in postnatal lethality of about 15% as well as between P1 and P22 was observed for the 129SV \times C57BL/6 genetic background. Because no difference in bodyweight was detected for embryos at E12.5, E15.5 or E18.5, the failure to thrive was most likely caused by reduced feeding capabilities. *PWScr^{m+/p-}* mice were fertile, bred in the expected Mendelian ratio and did not become obese at any point in time [42]. Expression of other genes in the PWS locus remained unaffected, except for a small decrease of the *Snord115* and *Ipw-G* exon expression [97].

In addition, magnetic resonance imaging revealed a decrease of grey-matter volume in the ventral hippocampus and septum areas of *PWScr^{m+/p-}* mice [89]. Orexin and melanin concentrating hormone systems in the lateral hippocampus were impaired in mutant mice, as the deletion of *Snord116* gene cluster causes a 60% reduction in orexin expressing neurons [88]. Consequently, expression of *pOx* (prepro-orexin) and *Peg3* (paternally imprinted gene 3) were significantly upregulated in *PWScr^{m+/p-}* [88]. The analysis of RNA-seq data led to the identification of >4000 differentially regulated genes in the hypothalamus of *PWScr^{m+/p-}* mice compared to wild-type controls [88]. Among the upregulated genes were those related to neurotransmitter transport, synaptic organization and cytokine production pathways [88]. *PWScr^{m+/p-}* mice also exhibited dysregulated “rapid eye movement” (REM) sleep, reduced peripheral thermoregulatory response, as well as an increase of peripheral body temperature compared to wild-type littermates during the light phase of the day. Those observations suggested that in addition to *Ndn*, *PWScr* derived non-protein coding RNAs also contribute to the regulation of sleep physiological measures in PWS [88].

11.2. The Second Mouse Model Harboring the Deletion of the PWS Critical Region (*Snord116del*)

The second mouse model featured an ~350 kb deletion of the *Snord116* gene cluster (UCSC, GRCm39/mm39 chr7:59,275,265-59,624,663—based on the location of genotyping primers). This eliminates an ~50 kb longer upstream region as opposed to the *PWScr^{m+/p-}* model (Figure 1C,D; Table 1) [43]. Gene targeting was performed by homologous recombination in BRUCE4 ES cells, thereby introducing *LoxP* sites flanking the *Snord116* gene array. Selected ES cell clones were injected into C57Bl/6J-Tyr^{c-2/J} albino blastocysts. Heterozygous offspring derived from the chimeras were mated with a transgenic C57BL/6J strain expressing Cre-recombinase. In a second experimental approach, targeted ES cells were transfected with a Cre expressing vector prior to blastocyst injection [43].

Offspring from both lines exhibited a similar phenotype and transmitted the paternal deletion through the germline. Although the entire cluster consisting of *Ipw-A* exons and *Snord116* genes was paternally deleted, the mouse model was named *Snord116del*. The expression of other genes in the PWS-locus remained unaffected by the deletion, except for the neighboring genes flanking the deletion. Thus, an approximate 35% decrease and a 33% increase in expression of *Snord107* and *Snord115* genes was observed, respectively [43]. Notably, this is in contrast to a slight decrease of the *Snord115* gene expression in *PWScr^{m+/p-}* mice compared to WT littermates [97]. Similarly, to the *PWScr^{m+/p-}* model, newborn *Snord116del^{m+/p-}* pups P0 harboring the paternally inherited deletion were indistinguishable from WT littermates. Growth retardation was detected from postnatal day 2 onwards.

In *Snord116del* mice, which were homozygous for the deletion (*Snord116del^{m-/p-}*), reduced bone and fat mass relative to their bodyweight accompanied by an increase in lean mass was reported [95]. *Snord116del* mice were fertile and bred normally, although the female sexual maturation was delayed. Interestingly, postnatal lethality was not reported for this *Snord116del* model and mice were healthy during the 18-month observation. It was hypothesized that the failure to thrive was due to hypotonia and insufficient suckling, but neither hypotonia nor empty stomachs were observed in *Snord116del* pups. However, the livers and stomachs of *Snord116del* pups weighed less at P5 and P13 than those of their WT

littermates, which might indicate a decreased rather than absent milk intake. An overall decreased stomach weight was also observed in the *PWScr^{m+/p-}* model, but the effect was not statistically significant when the reduced bodyweight of the animals was taken into account (Skryabin et al., unpublished). *Igf1* levels were significantly lower in mice lacking *Snord116* expression, although there were no detectable anomalies of the pituitary gland itself [43].

The onset of locomotive abilities was delayed in *Snord116del* mice; yet, no differences in motor abilities were detected when reflex-related tasks were tested [90]. Furthermore, *Snord116del* mice exhibited an impairment in the recognition of novel objects and the memory of object location. In addition, the mice demonstrated a tendency towards increased anxiety-related behavior.

Food consumption was normal in the paternally deleted *Snord116del^{m+/p-}* mice, both on regular chow and high-fat diet. Indeed, the mutants were even somewhat resistant to obesity, as— compared to WT siblings—they displayed significantly lower bodyfat percentages after 4 months on a high-fat diet [43]. Despite these findings, initial analysis of *Snord116del^{m+/p-}* mice revealed an increase in food intake relative to their lower bodyweight, which was interpreted as hyperphagia [43]. Forthcoming studies revealed altered diurnal energy regulation in *Snord116del* mice, thereby showing decreased respiratory exchange rates (a result of increased fat oxidation as opposed to carbohydrate) during the 12-h light period [94]. Ghrelin levels in *Snord116del* with *ad libitum* access to food were significantly increased and comparable to the level observed in WT mice after a 24h fast, whereas insulin sensitivity was normal in mutant females but increased in males [94]. In late adulthood (28–34 weeks of age), increased glucose tolerance and insulin sensitivity were detected independent of *Snord116del^{m-/p-}* gender [95]. *Snord116del^{m-/p-}* mice exhibited ~11% and ~31% higher calories per gram of bodyweight uptake in early (12–16 weeks of age) and late adulthood (28–34 weeks of age) [95]. In early adulthood, *Snord116del^{m-/p-}* mice showed lower activity levels during the 12-h dark phase and increased energy expenditure during the light phase. However, in late adulthood, this profile was inverted, leading to increased activity during the dark phase [95]. Core body temperature was also reduced in mutant mice in early adulthood. *Snord116del^{m-/p-}* mice were partially resistant to high fat diet-induced obesity, which subsequently, did not lead to a significant increase in bodyweight compared to normal chow, although the fat mass was increased [95]. In stark contrast, recent analysis uncovered that paternally inherited *Snord116del* mice displayed no significant differences (compared to the WT controls) in the 24-h food intake of animals that had *ad libitum* access or those following a 24-h fast [91]. However, when the *Snord116* cluster was specifically eliminated in the mediobasal hypothalamus of adult mice, hyperphagia leading to obesity in a subset of animals was detected [91].

However, when the *Snord116del*-based model harboring a mosaic partial deletion of the *Snord116* gene cluster was investigated in adult animals, the 16% reduction of *Snord116* expression did not result in any significant effect on bodyweight. In addition, no remarkable change in weight of any major tissue/organ or even the lean mass was identified [96]. Reduction of *Snord116* expression resulted in an increase of small white adipose tissue mass; yet, food intake was reduced during *ad libitum* food access or after a 48-h fast [96]. The mosaic mice displayed an impaired glucose clearance rate and insulin resistance at 13 weeks of age [96]. There was no detectable difference in energy expenditure or respiratory exchange rate, only a short time delay during the transition from the light, somnolent phase to the dark, active phase.

Changes in expression profiles of selected genes were investigated in *Snord116del* mice by various research groups. The analysis of genes representing the leptin/melanocortin pathway revealed inconsistent results. Some approaches uncovered no altered expression profiles for *Npy* (neuropeptide Y), *Lepr* (leptin receptor), *Agr* (agouti-related protein), *Pomc* (Proopiomelanocortin), *Pcsk1* (prohormone convertase 1) or its transcription activator *Nhlh2* (nescient helix-loop-helix 2) genes [91]. However, early reports demonstrated reduced expression levels of *Pcsk1* and *Nhlh2* genes and a shift in the ratio of active to inactive

precursor forms of circulating hormones, e.g., proinsulin-insulin, preproghrelin-ghrelin, an effect which is presumably due to the impairment of the necessary processing pathway [93]. The same group also reported a significant increase of *Npy* and *Agr* expression in *Snord116del* mice after refeeding. The *Snord116* deletion also leads to an impairment of pancreatic development, resulting in a reduction of pancreatic islet size and a decrease of *insulin 1(Ins1)* and *insulin 2(Ins2)* gene expression [92]. In addition, expression of *Pdx1*, *Pax6* and *Nkx6-1* transcription factors, which are important for pancreatic development, was downregulated in adult *Snord116del* mice. In the cerebellum of *Snord116del* at postnatal day 30, the mean cell body diameter of Purkinje neurons was reduced by 21%. In the cortex of *Snord116del* mice, the number of diurnal differentially methylated regions was dramatically reduced, with only 3% of regions showing the same rhythmic methylation pattern that is present in wild-type mice [132]. Among those genes that were epigenetically dysregulated in *Snord116del* mice, functional clusters regulating the circadian entrainment, AMPK (AMP-activated Protein Kinase) signaling, stem cell pluripotency, axon guidance, insulin resistance and dopaminergic synapse function were identified. Interestingly, in *Snord116del* mice, altered diurnal methylation of the imprinted *Dlk1-Dio3* locus and upregulation of its maternally expressed genes were reported, suggesting putative “cross-talk” between two imprinted loci [132].

Results obtained from the *Snord116* KO models are in accordance with the current leading hypothesis that the absence of *SNORD116* gene clusters indeed plays a causative role in the early onset of PWS pathogenesis. *SNORD116* genomic regions became a prime focus following the discovery of PWS patients harboring a rare minimal deletion of the *SNORD116* gene cluster (Figure 1A) [34–39].

Despite the fact that the IPW-A exons show little sequence conservation among mammals, we cannot completely rule out functional roles of exon-derived large non-protein coding RNAs in the *PWScr* region. Since *SNORD116* genes from this cluster are the only genes from this region that exhibit a high degree of sequence similarities between different mammals, most research is aimed at elucidating their function. However, the *PWScr* region, as part of a long non-protein coding U-UBE3A-AS transcript, also encodes IPW-A exons; yet, the functional significance of *SNORD116* or non-protein coding IPW-A exons, or the roles of both in the pathogenesis of PWS are yet to be elucidated.

12. Snord115 Gene Cluster

SNORD115 is another large, imprinted gene cluster identified within the PWS locus (Figure 1). Historically, it was the first snoRNA with a presumed mRNA target. The antisense element within the snoRNA exhibits an 18 nt long evolutionarily conserved complementarity to the alternatively spliced exon Vb of the 5-HT_{2C} serotonin receptor pre-mRNA that is also subject of posttranscriptional A-to-I editing (Figure 3). The 5-HT_{2C} receptor is part of many complex regulatory networks that, amongst others, have been linked to obesity, feeding behavior, mental state, sleep cycles, autism, neuropsychiatric disorders (e.g., schizophrenia, depression) and neurodegenerative diseases (e.g., Parkinson, Alzheimer) [133,134]. Alternative splicing of exon V of the 5-HT_{2C} receptor pre-mRNA results in an inactive, truncated variant of the receptor. The efficacy of 5-HT_{2C} G-protein coupling is regulated via posttranscriptional A-to-I editing of the pre-mRNA within the exon Vb region, which generates over 32 different 5-HT_{2C} mRNA isoforms that collectively modulate the serotonergic signal transduction to varying degrees [135,136]. Ex vivo experiments in HEK293 or Neuro2A cells demonstrated that *SNORD115* can interfere with alternative splicing of the 5-HT_{2C} serotonin receptor pre-mRNA. However, this was only observed when the original splice site of pre-mRNA had been mutated for optimal splicing [137]. Studies examining the *PWS-IC^{m+/pΔ35kb}* mouse model that express barely detectable levels of *Snord115*, revealed conflicting results. Initially, it was suggested that the absence of *Snord115* RNA did not affect alternative splicing of 5-HT_{2C} pre-mRNA [83]. However, more recently, the same group reported increased expression of the truncated receptor isoform in the hypothalamus of *PWS-IC^{m+/pΔ35kb}* mice [138]. In

mice, Snord115 is expressed in neurons but is entirely absent from the choroid plexus, an area where 5-Ht2cr mRNA is abundant. RNA deep sequencing analysis of choroid plexus samples from a mouse model with ectopic Snord115 expression revealed that Snord115 is not involved in the regulation of 5-Ht2cr pre-mRNA alternative splicing *in vivo* [139]. Recently, a long-awaited mouse model harboring the paternal deletion of the *Snord115* gene cluster in the C57BL/6J genetic background was reported (Figure 1C,D; Table 1) [44]. RNA deep sequencing of different brain areas revealed that the lack of Snord115 expression does not alter alternative splicing of 5-Ht2cr pre-mRNA [44]. Likewise, transcriptome analysis of hypothalamus samples from PWS patients did not detect differences in 5-HT2CR pre-mRNA splicing [140].

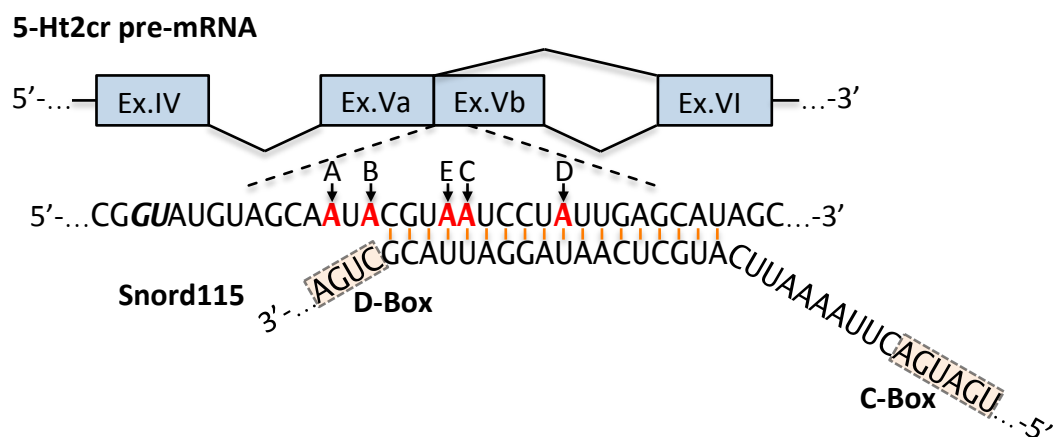


Figure 3. Schematic representation of 5-Ht2cr pre-mRNA exons IV to VI and putative targeting region of Snord115 within exon Vb (drawings are not to scale). Alternative splicing site (GU) of 5-Ht2cr pre-mRNA exon Vb is indicated with bold italic letters. A-to-I editing sites A–D are denoted in red and labeled with arrows, accordingly. Snord115 C- and D-boxes are highlighted [128,139].

In addition, potential SNORD115 functions in the regulation of 5-Ht2cr pre-mRNA posttranscriptional A-to-I editing were explored. *Ex vivo* experiments in cell culture demonstrated that Snord115 can interfere with RNA editing if an atypically nucleolar-localized mRNA substrate is present [141]. The analysis of the “autistic” mouse model, which harbors a paternal duplication of the PWS-locus imprinted genes (patDp/+ mouse) and *PWS-IC^{m+/pΔ35kb}* mice reported an increase of A-to-I editing of 5-Ht2cr pre-mRNA [83,142]. However, both studies lack sufficient sequencing depth and are controversial due to differences in Snord115 expression levels (~2-fold increase in patDp/+ mice and almost no expression in *PWS-IC^{m+/pΔ35kb}* mice) [83,142]. The analysis of mouse models with ectopic expression of *Snord115* in the choroid plexus suggested the formation of a double-stranded structure between Snord115 and exon Vb of 5-Ht2cr pre-mRNA, which may also be subject to ADAR (Adenosine deaminases acting on RNA)-mediated A-to-I editing, i.e., similar to the intramolecular duplex formed by exon Vb and the downstream intron of 5-Ht2cr pre-mRNA [139]. Consequently, analysis of 5-Ht2cr pre-mRNA revealed only a modestly reduced A-to-I editing at major sites, questioning the overall biological significance of the Snord115-5Ht2c receptor pre-mRNA interaction and its contribution to PWS pathophysiology [139]. A mouse model with a paternal deletion of the *Snord115* gene cluster also revealed only modest alterations in 5-Ht2cr mRNA editing profiles [44]; moreover, differences were detected in a brain region-specific manner. The functional significance of these minor changes remains to be resolved, as mice showed no obvious phenotypic abnormalities, they bred normally, displayed normal growth patterns and energy balance on either a normal chow or high fat diet. There were no noticeable differences in social or emotional behavioral phenotypes associated with altered 5-Ht2c receptor regulation [44]. Therefore, a functional interaction of *Snord115* with pre-mRNA or mRNA targets, should be considered fortuitous, until there is sound *in vivo* evidence [143]. This stretch of comple-

mentarity is rather testimony to the manner in which sequences of genomes evolve, namely by duplicating existing genetic material and deletions and not by out of the blue de novo generation. As a result, the sequence of genomes is much less complex than theoretically possible, alone due to the presence of at least 50% repetitive elements, e.g., in humans [144].

13. PWS Compensation Models

Genetically modified mouse models and the identification of PWS patients with rare small deletions helped to pinpoint the minimal PWS critical region (*PWScr*) to the *SNORD116/IPW-A* genomic region. However, an important question remained unanswered. Is the deletion of genomic DNA harboring unknown regulatory elements or is the lack of non-protein coding RNA expression causative of PWS in patients? Therefore, additional mouse models were generated, in which non-protein coding RNA(s) of *PWScr* was re-introduced into expression-lacking animals that exhibited a typical PWS-like phenotype. As the *SNORD116* genes within the *PWScr* region exhibit the highest degree of sequence similarity between different mammalian species, most effort had been devoted to understanding their functions. Two *Snord116* transgenic mouse lines expressing snoRNA embedded in introns of different host genes were generated (Table 1). The first model contained a single copy transgenic *Snord116* within nucleolin intron 11 driven by a neural-specific enolase promoter. This transgene was crossed with a PWS knockout mouse line containing a deletion from *Snrpn* to *Ube3a*, encompassing the complete *PWScr* [142]. Expression from the transgene failed to rescue either the neonatal lethality or growth retardation of mice with the paternal inheritance of the deletion. These negative results were explained by potentially insufficient expression levels of the single copy gene compared to the highly abundant endogenous *Snord116* RNA transcribed from a cluster containing over 66 repeats.

The second model (TgSnord116) was generated by expressing two copies of mouse *Snord116* and one copy of rat *Snord116* from the introns of an *eGFP* host gene [97]. Transgenic mice were crossed with a *PWScr^{m+/p-}* mouse model, resulting in *PWScr^{m+/p-}*-TgSnord116 animals. Transgene expression of *Snord116* did not compensate the growth retardation phenotype observed in the *PWScr^{m+/p-}* model [97]. A possible explanation could be the tissue-specific expression of the transgenic *eGFP* construct, which was absent in thalamus, hypothalamus, midbrain and pons of *PWScr^{m+/p-}*-TgSnord116 mice [97]. Because dysregulation of the hypothalamic endocrine system is associated with PWS in humans, one would expect that absence of *Snord116* expression in this tissue could contribute to growth retardation in mice [145,146]. Consequently, the important question of the functional significance of *Snord116* in PWS still needed to be addressed by generating compensatory transgenic animals that express *Snord116* in the same brain regions as wild-type mice.

In an attempt to achieve a sufficient expression level of transgenic *Snord116* in the *Snord116del^{m+/p-}* knockout model, a transgene carrying multiple copies of *Snord116* and *Ipw-A* exons was designed to mimic the original gene organization (Table 1) [98]. The transgene construct contained three complete *PWScr* repeat units under the control of a cytomegalovirus (CMV) promoter. Each repeat contained an intron located *Snord116* copy embedded by *Ipw-A* exons. Pronuclear injection of fertilized oocytes with the engineered DNA construct resulted in transgenic mice putatively with head-to-tail donor DNA integration, which often occurs during knock-in or transgene generation [147,148]. The construct was integrated nine times in the genome, resulting in a total of 27 copies of *Snord116* [98]. The insertion was identified at chromosomal region 7qE3 about 47 Mb away from the *PWScr* region. The resulting transgene failed to express *Snord116* and *Ipw-A* exons on a *Snord116del^{m+/p-}* knockout background and hence, to rescue the growth retardation phenotype [98].

In an attempt to re-introduce *Snord116* RNAs into the hypothalamus of adult *Snord116del* mouse models (*Snord116del^{m-/p-}*) at different ages, an AAV vector expressing a single *Snord116* copy was injected into *Snord116del^{m-/p-}* male mice (Table 1) [100]. Apparently, no significant effects were observed, except for a slight increase in energy expenditure when

compared to the vehicle-injected *Snord116del^{m-/p-}* control mice, as well as a reduced rate of weight gain. The effect of the viral *Snord116* expression in knockout animals was rather low and also highly dependent on the age of treated mice and region of injection, generally favoring younger mice and those that were injected in the mid- (rather than anterior) region of the hypothalamus [100]. However, lack of *Snord116* expression quantification from the AAV vector together with putative differences observed at various time points of virus microinjections raised questions about the application and potential efficacy of AAV mediated gene therapy for PWS patients.

An alternative strategy was to inactivate the PWS imprinting center on the maternal chromosome (Table 1). To do this, the effects of maternal transmission of the 4.8 kb IC and exon 1 *Snrpn* deletion were studied [99]. Maternal inheritance of the deletion resulted in active expression of both protein coding and non-protein coding genes in the PWS locus from the maternal allele in mice whose expression of the paternal allele was impaired due to either a short 4.8 kb deletion on the IC-center at the paternal *PWS-IC^{mΔ4.8kb/pΔ4.8kb}* allele or due to a large chromosomal deletion from *Snrpn* exon 2 to the *Ube3a* gene—*PWS-IC^{mΔ4.8kb/pΔS-U}*. Remarkably, the maternal expression was able to rescue the prominent postnatal lethality phenotype in both the small (survival rate *PWS-IC^{m+/pΔS-U}*: 56%, *PWS-IC^{mΔ4.8kb/pΔS-U}*: 96%) and large (*PWS-IC^{m+/pΔS-U}*: 0%, *PWS-IC^{mΔ4.8kb/pΔS-U}*: 96%) deletions. Growth retardation was also compensated and the bodyweights of mice inheriting the additional maternal Δ4.8 kb deletion showed no statistically significant difference from their WT littermates by the age of 6 weeks. This was achieved despite the fact that expression levels of the imprinted genes *Snrpn* (21%–35%), *Snord116* (8%), *Snord115* (10%), and *Ndn* (28%) from the maternal Δ4.8 kb allele were significantly lower compared to wild-type mice [99].

Another strategy applied was the re-activation of imprinted *PWScr* non-protein coding genes from the maternal allele by insertion of the regulatory *LoxP* cassette 5'- to the *Snord116* gene cluster in the *PWScr^{m+/p-}* mouse model (Table 1) [97]. The *PWScr^{m5'LoxP/p-}* mice showed a mild growth delay between postnatal day 7 and 19, but over time, gained more weight than their *PWScr^{m+/p-}* siblings; weight differences to wild-type littermates became insignificant by postnatal day 21. Although the expression levels of *Snord116* and *Ipw-A* non-protein coding RNAs from the maternal allele were reduced by 7.5 and 12-fold, respectively, it apparently was sufficient to rescue the growth retardation phenotype. The inserted 5'*LoxP* cassette in *PWScr^{m5'LoxP/p-}* mice results in ubiquitous transcriptional activation of *Snord116* and *Snord115* gene clusters from the maternal allele. Expression of *Snord64* RNA and protein coding genes at the PWS locus was not perturbed. Although *Snord116* was detected in the glial cells of *PWScr^{m5'LoxP/p-}* mice, the overall brain areas with neuronal snoRNA expression between KI and wild type mice was quite similar [97]. This was the first experimental evidence showing that expression of non-protein coding RNAs is primarily causative of growth retardation in mice and potentially PWS in patients. However, the functional significance of the *Snord116* or long RNAs consisting of alternatively spliced *Ipw-A* exons in the *PWScr* locus or both RNAs is yet to be investigated [97].

14. Conclusions

Despite over two decades of investigations, we still lack an in vivo animal model that adequately displays the entire spectrum of PWS symptoms, especially during the second phase that includes obesity. The data supporting a hyperphagic, adult-onset obesity phenotype in mice remains weak at best, with researchers reporting conflicting results despite having used the same knockout strain [43,91]. While some of the conflicting results could be explained by the different methods used to normalize food consumption to respective body weight, this is a far cry from the late-stage morbid obesity observed in patients. This not only shapes the public perception of the disease; it is also the main underlying factor for increased mortality [20].

In general, the differences between various animal models that affect the same gene must also be scrutinized. The use of experimental animals with various genetic back-

grounds is known to lead to significant phenotypic differences (see for example [149]). There are experimental, even interpretational variances between laboratories leading to reports of different phenotypes. In different models of gene depleted animals, the target gene is only partially inactivated. If this results, for example, in the expression of a defective (e.g., truncated) gene product, the latter may convey “side” effects. Alternatively, a truncated gene product (or one “rescued” by splicing) still might be functional to various degrees. Finally, off target events, e.g., during propagation in cell culture is a scary but rarely recognized possibility of observing different phenotypes.

Modelling of PWS in mice is complicated by the complexity of the affected region itself, which spans more than 1.5 Mb and contains several genes, quite a few with an associated phenotype of their own. At least for the protein-coding genes, the sequence similarity between mice and humans seems to correlate with functional similarity, as the respective mouse models display a comparable phenotype [33]. The vast majority of human patients are affected by a disruption of these genes in addition to loss of the functionally elusive non-protein coding RNAs and transcripts. The existing mouse models led to a better understanding of the underlying pathophysiological mechanisms and some were tested within a number of ongoing pharmacological trials in search of therapeutic agents [150].

For the non-protein coding transcripts, it is more complicated still. Their mechanistic function is unknown, although all insights gained thus far suggest that they are of importance in both species [151]. Since even rare, small deletions in human patients encompassing nothing more than non-protein coding genes results in the manifestation of core symptoms typical to PWS, further research focusing on the PWS_{cr} region with emphasis on the encoded RNAs and transcripts should eventually elucidate a causative mechanism of the disease [34–39].

The first generation of compensatory models are in agreement with the identification of the minimal critical region responsible for the PWS phenotype in mice. One of the important insights gained from those models is that transcript localization, proper processing and quantity—but only to a certain degree [97]—are of vital importance. This should be taken into account for prospective models; for example, the natural organization of respective genes should be mimicked as a tandemly repetitive cluster. Moreover, the successful re-activation of the imprinted maternal allele proved to be an option if and when the necessary genome-editing methods are refined enough and deemed safe for human application. This could become a feasible therapeutic strategy and an elegant solution for all patients regardless of respective cause, i.e., deletion or maternal uniparental disomy (UPD), since at least one functional allele is always present.

Author Contributions: All authors contributed to the literature search and the layout of the manuscript. All authors have read and agreed to the published version of the manuscript.

Funding: This work was supported by the Deutsche Forschungsgemeinschaft (DFG) (RO5622/1-1 to TSR and SK259/2-1 to BVS).

Acknowledgments: We thank Stephanie Klco-Brosius for manuscript editing. We apologize to those researches whose contributions could not be cited due to the space limitations.

Conflicts of Interest: The authors declare no conflict of interest.

References

1. McCandless, S.E. Clinical report—Health supervision for children with Prader-Willi syndrome. *Pediatrics* **2011**, *127*, 195–204. [[CrossRef](#)]
2. Cassidy, S.B.; Schwartz, S.; Miller, J.L.; Driscoll, D.J. Prader-Willi syndrome. *Genet. Med.* **2012**, *14*, 10–26. [[CrossRef](#)]
3. Kalsner, L.; Chamberlain, S.J. Prader-Willi, Angelman, and 15q11-q13 Duplication Syndromes. *Pediatr. Clin. N. Am.* **2015**, *62*, 587–606. [[CrossRef](#)]
4. Angulo, M.A.; Butler, M.G.; Cataletto, M.E. Prader-Willi syndrome: A review of clinical, genetic, and endocrine findings. *J. Endocrinol. Invest.* **2015**, *38*, 1249–1263. [[CrossRef](#)]
5. Butler, M.G.; Miller, J.L.; Forster, J.L. Prader-Willi Syndrome—Clinical Genetics, Diagnosis and Treatment Approaches: An Update. *Curr. Pediatr. Rev.* **2019**, *15*, 207–244. [[CrossRef](#)]

6. Rocha, C.F.; Paiva, C.L. Prader-Willi-like phenotypes: A systematic review of their chromosomal abnormalities. *Genet. Mol. Res.* **2014**, *13*, 2290–2298. [[CrossRef](#)]
7. Kim, S.J.; Miller, J.L.; Kuipers, P.J.; German, J.R.; Beaudet, A.L.; Sahoo, T.; Driscoll, D.J. Unique and atypical deletions in Prader-Willi syndrome reveal distinct phenotypes. *Eur. J. Hum. Genet.* **2012**, *20*, 283–290. [[CrossRef](#)] [[PubMed](#)]
8. Miller, J.L.; Lynn, C.H.; Driscoll, D.C.; Goldstone, A.P.; Gold, J.A.; Kimonis, V.; Dykens, E.; Butler, M.G.; Shuster, J.J.; Driscoll, D.J. Nutritional phases in Prader-Willi syndrome. *Am. J. Med. Genet. Part A* **2011**, *155*, 1040–1049. [[CrossRef](#)] [[PubMed](#)]
9. Kanaka-Gantenbein, C.; Kogia, C.; Abdel-Naser, M.B.; Chrousos, G.P. Skin manifestations of growth hormone-induced diseases. *Rev. Endocr. Metab. Disord.* **2016**, *17*, 259–267. [[CrossRef](#)] [[PubMed](#)]
10. Crinò, A.; Fintini, D.; Bocchini, S.; Grugni, G. Obesity management in Prader-Willi syndrome: Current perspectives. *Diabetes Metab. Syndr. Obes.* **2018**, *11*, 579–593. [[CrossRef](#)]
11. Dykens, E.M.; Roof, E.; Hunt-Hawkins, H.; Daniell, C.; Jurgensmeyer, S. Profiles and trajectories of impaired social cognition in people with Prader-Willi syndrome. *PLoS ONE* **2019**, *14*, e0223162. [[CrossRef](#)] [[PubMed](#)]
12. Costa, R.A.; Ferreira, I.R.; Cintra, H.A.; Gomes, L.H.F.; Guida, L.D.C. Genotype-Phenotype Relationships and Endocrine Findings in Prader-Willi Syndrome. *Front. Endocrinol.* **2019**, *10*, 864. [[CrossRef](#)] [[PubMed](#)]
13. Cheon, C.K. Genetics of Prader-Willi syndrome and Prader-Will-Like syndrome. *Ann. Pediatr. Endocrinol. Metab.* **2016**, *21*, 126–135. [[CrossRef](#)] [[PubMed](#)]
14. Driscoll, D.J.; Miller, J.L.; Schwartz, S.; Cassidy, S.B. Prader-Willi Syndrome. In *GeneReviews*[®] [Internet]; University of Washington: Seattle, DC, USA, 2017.
15. Lionti, T.; Reid, S.M.; White, S.M.; Rowell, M.M. A population-based profile of 160 Australians with Prader-Willi syndrome: Trends in diagnosis, birth prevalence and birth characteristics. *Am. J. Med. Genet. Part A* **2015**, *167*, 371–378. [[CrossRef](#)]
16. Vogels, A.; Van Den Ende, J.; Keymolen, K.; Mortier, G.; Devriendt, K.; Legius, E.; Fryns, J.P. Minimum prevalence, birth incidence and cause of death for Prader-Willi syndrome in Flanders. *Eur. J. Hum. Genet.* **2004**, *12*, 238–240. [[CrossRef](#)]
17. Butler, J.V.; Whittington, J.E.; Holland, A.J.; Boer, H.; Clarke, D.; Webb, T. Prevalence of, and risk factors for, physical ill-health in people with Prader-Willi syndrome: A population-based study. *Dev. Med. Child Neurol.* **2002**, *44*, 248–255. [[CrossRef](#)]
18. Butler, M.G.; Manzardo, A.M.; Heinemann, J.; Loker, C.; Loker, J. Causes of death in Prader-Willi syndrome: Prader-Willi Syndrome Association (USA) 40-year mortality survey. *Genet. Med.* **2017**, *19*, 635–642. [[CrossRef](#)]
19. Pacoricona Alfaro, D.L.; Lemoine, P.; Ehlinger, V.; Molinas, C.; Diene, G.; Valette, M.; Pinto, G.; Coupaye, M.; Poitou-Bernert, C.; Thuilleaux, D.; et al. Causes of death in Prader-Willi syndrome: Lessons from 11 years' experience of a national reference center. *Orphanet J. Rare Dis.* **2019**, *14*, 238. [[CrossRef](#)]
20. Proffitt, J.; Osann, K.; McManus, B.; Kimonis, V.E.; Heinemann, J.; Butler, M.G.; Stevenson, D.A.; Gold, J.A. Contributing factors of mortality in Prader-Willi syndrome. *Am. J. Med. Genet. A.* **2019**, *179*, 196–205. [[CrossRef](#)]
21. Grugni, G.; Sartorio, A.; Crinò, A. Growth hormone therapy for Prader-willi syndrome: Challenges and solutions. *Ther. Clin. Risk Manag.* **2016**, *12*, 873–881. [[CrossRef](#)]
22. Frixou, M.; Vlek, D.; Lucas-Herald, A.K.; Keir, L.; Kyriakou, A.; Shaikh, M.G. The use of growth hormone therapy in adults with Prader-Willi syndrome: A systematic review. *Clin. Endocrinol.* **2020**. [[CrossRef](#)]
23. Harris, R.M.; Stafford, D.E.J. Prader Willi syndrome: Endocrine updates and new medical therapies. *Curr. Opin. Endocrinol. Diabetes Obes.* **2020**, *27*, 56–62. [[CrossRef](#)] [[PubMed](#)]
24. Tan, Q.; Orsso, C.E.; Deehan, E.C.; Triador, L.; Field, C.J.; Tun, H.M.; Han, J.C.; Müller, T.D.; Haqq, A.M. Current and emerging therapies for managing hyperphagia and obesity in Prader-Willi syndrome: A narrative review. *Obes. Rev.* **2020**, *21*, e12992. [[CrossRef](#)] [[PubMed](#)]
25. Nicholls, R.D.; Knoll, J.H.; Butler, M.G.; Karam, S.; Lalande, M. Genetic imprinting suggested by maternal heterodisomy in nondeletion Prader-Willi syndrome. *Nature* **1989**, *342*, 281–285. [[CrossRef](#)]
26. Butler, M.G. Genomic imprinting disorders in humans: A mini-review. *J. Assist. Reprod. Genet.* **2009**, *26*, 477–486. [[CrossRef](#)] [[PubMed](#)]
27. Wawrzik, M.; Unmehopa, U.A.; Swaab, D.F.; van de Nes, J.; Buiting, K.; Horsthemke, B. The C15orf2 gene in the Prader-Willi syndrome region is subject to genomic imprinting and positive selection. *Neurogenetics* **2010**, *11*, 153–161. [[CrossRef](#)] [[PubMed](#)]
28. Bhoj, E.J.; Rajabi, F.; Baker, S.W.; Santani, A.; Tan, W.H. Imprinted genes in clinical exome sequencing: Review of 538 cases and exploration of mouse-human conservation in the identification of novel human disease loci. *Eur. J. Med. Genet.* **2020**, *63*, 103903. [[CrossRef](#)]
29. Spikol, E.D.; Laverriere, C.E.; Robnett, M.; Carter, G.; Wolfe, E.M.; Glasgow, E. Zebrafish Models of Prader-Willi Syndrome: Fast Track to Pharmacotherapeutics. *Diseases* **2016**, *4*, 13. [[CrossRef](#)]
30. Van Amerongen, R.; Nawijn, M.; Franca-Koh, J.; Zevenhoven, J.; van der Gulden, H.; Jonkers, J.; Berns, A. Frat is dispensable for canonical Wnt signaling in mammals. *Genes Dev.* **2005**, *19*, 425–430. [[CrossRef](#)] [[PubMed](#)]
31. Neumann, L.C.; Feiner, N.; Meyer, A.; Buiting, K.; Horsthemke, B. The imprinted NPAP1 gene in the Prader-Willi syndrome region belongs to a POM121-related family of retrogenes. *Genome Biol. Evol.* **2014**, *6*, 344–351. [[CrossRef](#)]
32. Neumann, L.C.; Markaki, Y.; Mladenov, E.; Hoffmann, D.; Buiting, K.; Horsthemke, B. The imprinted NPAP1/C15orf2 gene in the Prader-Willi syndrome region encodes a nuclear pore complex associated protein. *Hum. Mol. Genet.* **2012**, *21*, 4038–4048. [[CrossRef](#)] [[PubMed](#)]

33. Bervini, S.; Herzog, H. Mouse models of Prader-Willi Syndrome: A systematic review. *Front. Neuroendocrinol.* **2013**, *34*, 107–119. [[CrossRef](#)] [[PubMed](#)]
34. Sahoo, T.; del Gaudio, D.; German, J.R.; Shinawi, M.; Peters, S.U.; Person, R.E.; Garnica, A.; Cheung, S.W.; Beaudet, A.L. Prader-Willi phenotype caused by paternal deficiency for the HBII-85 C/D box small nucleolar RNA cluster. *Nat. Genet.* **2008**, *40*, 719–721. [[CrossRef](#)]
35. De Smith, A.J.; Purmann, C.; Walters, R.G.; Ellis, R.J.; Holder, S.E.; Van Haelst, M.M.; Brady, A.F.; Fairbrother, U.L.; Dattani, M.; Keogh, J.M.; et al. A deletion of the HBII-85 class of small nucleolar RNAs (snoRNAs) is associated with hyperphagia, obesity and hypogonadism. *Hum. Mol. Genet.* **2009**, *18*, 3257–3265. [[CrossRef](#)] [[PubMed](#)]
36. Duker, A.L.; Ballif, B.C.; Bawle, E.V.; Person, R.E.; Mahadevan, S.; Alliman, S.; Thompson, R.; Traylor, R.; Bejjani, B.A.; Shaffer, L.G.; et al. Paternally inherited microdeletion at 15q11.2 confirms a significant role for the SNORD116 C/D box snoRNA cluster in Prader-Willi syndrome. *Eur. J. Hum. Genet.* **2010**, *18*, 1196–1201. [[CrossRef](#)] [[PubMed](#)]
37. Bieth, E.; Eddiry, S.; Gaston, V.; Lorenzini, F.; Buffet, A.; Conte Auriol, F.; Molinas, C.; Cailley, D.; Rooryck, C.; Arveiler, B.; et al. Highly restricted deletion of the SNORD116 region is implicated in Prader-Willi Syndrome. *Eur. J. Hum. Genet.* **2015**, *23*, 252–255. [[CrossRef](#)]
38. Fontana, P.; Grasso, M.; Acquaviva, F.; Gennaro, E.; Galli, M.L.; Falco, M.; Scarano, F.; Scarano, G.; Lonardo, F. SNORD116 deletions cause Prader-Willi syndrome with a mild phenotype and macrocephaly. *Clin. Genet.* **2017**, *92*, 440–443. [[CrossRef](#)]
39. Tan, Q.; Potter, K.J.; Burnett, L.C.; Orsso, C.E.; Inman, M.; Ryman, D.C.; Haqq, A.M. Prader-Willi-Like Phenotype Caused by an Atypical 15q11.2 Microdeletion. *Genes* **2020**, *11*, 128. [[CrossRef](#)]
40. Gabriel, J.M.; Merchant, M.; Ohta, T.; Ji, Y.; Caldwell, R.G.; Ramsey, M.J.; Tucker, J.D.; Longnecker, R.; Nicholls, R.D. A transgene insertion creating a heritable chromosome deletion mouse model of Prader-Willi and angelman syndromes. *Proc. Natl. Acad. Sci. USA* **1999**, *96*, 9258–9263. [[CrossRef](#)]
41. Tsai, T.-F.; Jiang, Y.; Bressler, J.; Armstrong, D.; Beaudet, A.L. Paternal Deletion from Snrpn to Ube3a in the Mouse Causes Hypotonia, Growth Retardation and Partial Lethality and Provides Evidence for a Gene Contributing to Prader-Willi Syndrome. *Hum. Mol. Genet.* **1999**, *8*, 1357–1364. [[CrossRef](#)]
42. Skryabin, B.V.; Gubar, L.V.; Seeger, B.; Pfeiffer, J.; Handel, S.; Robeck, T.; Karpova, E.; Rozhdestvensky, T.S.; Brosius, J. Deletion of the MBII-85 snoRNA gene cluster in mice results in postnatal growth retardation. *PLoS Genet.* **2007**, *3*, e235. [[CrossRef](#)]
43. Ding, F.; Li, H.H.; Zhang, S.; Solomon, N.M.; Camper, S.A.; Cohen, P.; Francke, U. SnoRNA Snord116 (Pwcr1/MBII-85) deletion causes growth deficiency and hyperphagia in mice. *PLoS ONE.* **2008**, *3*, e1709. [[CrossRef](#)]
44. Hebras, J.; Marty, V.; Personnaz, J.; Mercier, P.; Krogh, N.; Nielsen, H.; Aguirrebengoa, M.; Seitz, H.; Pradere, J.P.; Guiard, B.P.; et al. Reassessment of the involvement of Snord115 in the serotonin 2c receptor pathway in a genetically relevant mouse model. *eLife* **2020**, *9*. [[CrossRef](#)] [[PubMed](#)]
45. Yang, T.; Adamson, T.E.; Resnick, J.L.; Leff, S.; Wevrick, R.; Francke, U.; Jenkins, N.A.; Copeland, N.G.; Brannan, C.I. A mouse model for Prader-Willi syndrome imprinting-centre mutations. *Nat. Genet.* **1998**, *19*, 25–31. [[CrossRef](#)] [[PubMed](#)]
46. Bressler, J.; Tsai, T.F.; Wu, M.Y.; Tsai, S.F.; Ramirez, M.A.; Armstrong, D.; Beaudet, A.L. The SNRPN promoter is not required for genomic imprinting of the Prader-Willi/Angelman domain in mice. *Nat. Genet.* **2001**, *28*, 232–240. [[CrossRef](#)] [[PubMed](#)]
47. Dubose, A.J.; Smith, E.Y.; Yang, T.P.; Johnstone, K.A.; Resnick, J.L. A new deletion refines the boundaries of the murine Prader-Willi syndrome imprinting center. *Hum. Mol. Genet.* **2011**, *20*, 3461–3466. [[CrossRef](#)]
48. Gérard, M.; Hernandez, L.; Wevrick, R.; Stewart, C.L. Disruption of the mouse necdin gene results in early post-natal lethality. *Nat. Genet.* **1999**, *23*, 199–202. [[CrossRef](#)]
49. Kuwako, K.; Hosokawa, A.; Nishimura, I.; Uetsuki, T.; Yamada, M.; Nada, S.; Okada, M.; Yoshikawa, K. Disruption of the paternal necdin gene diminishes TrkA signaling for sensory neuron survival. *J. Neurosci.* **2005**, *25*, 7090–7099. [[CrossRef](#)]
50. Muscatelli, F.; Abrous, D.N.; Massacrier, A.; Boccaccio, I.; Le Moal, M.; Cau, P.; Cremer, H. Disruption of the mouse Necdin gene results in hypothalamic and behavioral alterations reminiscent of the human Prader-Willi syndrome. *Hum. Mol. Genet.* **2000**, *9*, 3101–3110. [[CrossRef](#)] [[PubMed](#)]
51. Tsai, T.F.; Armstrong, D.; Beaudet, A.L. Necdin-deficient mice do not show lethality or the obesity and infertility of Prader-Willi syndrome. *Nat. Genet.* **1999**, *22*, 15–16. [[CrossRef](#)] [[PubMed](#)]
52. Schaller, F.; Watrin, F.; Sturny, R.; Massacrier, A.; Szepetowski, P.; Muscatelli, F. A single postnatal injection of oxytocin rescues the lethal feeding behaviour in mouse newborns deficient for the imprinted Magel2 gene. *Hum. Mol. Genet.* **2010**, *19*, 4895–4905. [[CrossRef](#)]
53. Kozlov, S.V.; Bogenpohl, J.W.; Howell, M.P.; Wevrick, R.; Panda, S.; Hogenesch, J.B.; Muglia, L.J.; Van Gelder, R.N.; Herzog, E.D.; Stewart, C.L. The imprinted gene Magel2 regulates normal circadian output. *Nat. Genet.* **2007**, *39*, 1266–1272. [[CrossRef](#)]
54. Li, C.; Lu, W.; Yang, L.; Li, Z.; Zhou, X.; Guo, R.; Wang, J.; Wu, Z.; Dong, Z.; Ning, G.; et al. MKRN3 regulates the epigenetic switch of mammalian puberty via ubiquitination of MBD3. *Natl. Sci. Rev.* **2020**, *7*, 671–685. [[CrossRef](#)]
55. Cattanaach, B.M.; Barr, J.A.; Evans, E.P.; Burtenshaw, M.; Beechey, C.V.; Leff, S.E.; Brannan, C.I.; Copeland, N.G.; Jenkins, N.A.; Jones, J. A candidate mouse model for Prader-Willi syndrome which shows an absence of Snrpn expression. *Nat. Genet.* **1992**, *2*, 270–274. [[CrossRef](#)] [[PubMed](#)]
56. Stefan, M.; Claiborn, K.C.; Stasiak, E.; Chai, J.H.; Ohta, T.; Longnecker, R.; Grealley, J.M.; Nicholls, R.D. Genetic mapping of putative Chrna7 and Luzzp2 neuronal transcriptional enhancers due to impact of a transgene-insertion and 6.8 Mb deletion in a mouse model of Prader-Willi and Angelman syndromes. *BMC Genom.* **2005**, *6*, 157. [[CrossRef](#)] [[PubMed](#)]

57. Stefan, M.; Ji, H.; Simmons, R.A.; Cummings, D.E.; Ahima, R.S.; Friedman, M.I.; Nicholls, R.D. Hormonal and metabolic defects in a prader-willi syndrome mouse model with neonatal failure to thrive. *Endocrinology* **2005**, *146*, 4377–4385. [[CrossRef](#)]
58. Stefan, M.; Simmons, R.A.; Bertera, S.; Trucco, M.; Esni, F.; Drain, P.; Nicholls, R.D. Global deficits in development, function, and gene expression in the endocrine pancreas in a deletion mouse model of Prader-Willi syndrome. *Am. J. Physiol. Endocrinol. Metab.* **2011**, *300*, E909–E922. [[CrossRef](#)]
59. Bischof, J.M.; Stewart, C.L.; Wevrick, R. Inactivation of the mouse Magel2 gene results in growth abnormalities similar to Prader-Willi syndrome. *Hum. Mol. Genet.* **2007**, *16*, 2713–2719. [[CrossRef](#)]
60. Mercer, R.E.; Wevrick, R. Loss of Magel2, a Candidate Gene for Features of Prader-Willi Syndrome, Impairs Reproductive Function in Mice. *PLoS ONE* **2009**, *4*, e4291. [[CrossRef](#)] [[PubMed](#)]
61. Mercer, R.E.; Kwolek, E.M.; Bischof, J.M.; van Eede, M.; Henkelman, R.M.; Wevrick, R. Regionally reduced brain volume, altered serotonin neurochemistry, and abnormal behavior in mice null for the circadian rhythm output gene Magel2. *Am. J. Med. Genet. B Neuropsychiatr. Genet.* **2009**, *150*, 1085–1099. [[CrossRef](#)]
62. Mercer, R.E.; Michaelson, S.D.; Chee, M.J.S.; Atallah, T.A.; Wevrick, R.; Colmers, W.F. Magel2 Is Required for Leptin-Mediated Depolarization of POMC Neurons in the Hypothalamic Arcuate Nucleus in Mice. *PLoS Genet.* **2013**, *9*, e1003207. [[CrossRef](#)]
63. Arble, D.M.; Pressler, J.W.; Sorrell, J.; Wevrick, R.; Sandoval, D.A. Sleeve gastrectomy leads to weight loss in the Magel2 knockout mouse. *Surg. Obes. Relat. Dis.* **2016**, *12*, 1795–1802. [[CrossRef](#)]
64. Maillard, J.; Park, S.; Croizier, S.; Vanacker, C.; Cook, J.H.; Prevot, V.; Tauber, M.; Bouret, S.G. Loss of Magel2 impairs the development of hypothalamic Anorexigenic circuits. *Hum. Mol. Genet.* **2016**, *25*, 3208–3215. [[CrossRef](#)]
65. Wijesuriya, T.M.; De Ceuninck, L.; Masschaele, D.; Sanderson, M.R.; Carias, K.V.; Tavernier, J.; Wevrick, R. The Prader-Willi syndrome proteins MAGEL2 and necdin regulate leptin receptor cell surface abundance through ubiquitination pathways. *Hum. Mol. Genet.* **2017**, *26*, 4215–4230. [[CrossRef](#)]
66. Oncul, M.; Dilsiz, P.; Ates Oz, E.; Ates, T.; Aklan, I.; Celik, E.; Sayar Atasoy, N.; Atasoy, D. Impaired melanocortin pathway function in Prader-Willi syndrome gene-Magel2 deficient mice. *Hum. Mol. Genet.* **2018**, *27*, 3129–3136. [[CrossRef](#)] [[PubMed](#)]
67. Baraghithy, S.; Smoum, R.; Drori, A.; Hadar, R.; Gammal, A.; Hirsch, S.; Gammal, A.; Hirsch, S.; Attar-Namdar, M.; Nemirovski, A.; et al. Magel2 Modulates Bone Remodeling and Mass in Prader-Willi Syndrome by Affecting Oleoyl Serine Levels and Activity. *J. Bone Miner. Res.* **2019**, *34*, 93–105. [[CrossRef](#)] [[PubMed](#)]
68. Crutcher, E.; Pal, R.; Naini, F.; Zhang, P.; Laugsch, M.; Kim, J.; Bajic, A.; Schaaf, C.P. mTOR and autophagy pathways are dysregulated in murine and human models of Schaaf-Yang syndrome. *Sci. Rep.* **2019**, *9*, 15935. [[CrossRef](#)]
69. Igarashi, M.; Narayanaswami, V.; Kimonis, V.; Galassetti, P.M.; Oveisi, F.; Jung, K.-M.; Piomelli, D. Dysfunctional oleoylethanolamide signaling in a mouse model of Prader-Willi syndrome. *Pharmacol. Res.* **2017**, *117*, 75–81. [[CrossRef](#)]
70. Luck, C.; Vitaterna, M.H.; Wevrick, R. Dopamine pathway imbalance in mice lacking Magel2, a Prader-Willi syndrome candidate gene. *Behav. Neurosci.* **2016**, *130*, 448–459. [[CrossRef](#)] [[PubMed](#)]
71. Ates, T.; Oncul, M.; Dilsiz, P.; Topcu, I.C.; Civas, C.C.; Alp, M.I.; Aklan, I.; Ates Oz, E.; Yavuz, Y.; Yilmaz, B.; et al. Inactivation of Magel2 suppresses oxytocin neurons through synaptic excitation-inhibition imbalance. *Neurobiol. Dis.* **2019**, *121*, 58–64. [[CrossRef](#)]
72. Chen, H.; Victor, A.K.; Klein, J.; Tacer, K.F.; Tai, D.J.; de Esch, C.; Nuttle, A.; Temirov, J.; Burnett, L.C.; Rosenbaum, M.; et al. Loss of MAGEL2 in Prader-Willi syndrome leads to decreased secretory granule and neuropeptide production. *JCI Insight* **2020**, *5*. [[CrossRef](#)]
73. Meziane, H.; Schaller, F.; Bauer, S.; Villard, C.; Matarazzo, V.; Riet, F.; Guillon, G.; Lafitte, D.; Desarmenien, M.G.; Tauber, M.; et al. An Early Postnatal Oxytocin Treatment Prevents Social and Learning Deficits in Adult Mice Deficient for Magel2, a Gene Involved in Prader-Willi Syndrome and Autism. *Biol. Psychiatry* **2015**, *78*, 85–94. [[CrossRef](#)]
74. Ieda, D.; Negishi, Y.; Miyamoto, T.; Johmura, Y.; Kumamoto, N.; Kato, K.; Miyoshi, I.; Nakanishi, M.; Ugawa, S.; Oishi, H.; et al. Two mouse models carrying truncating mutations in Magel2 show distinct phenotypes. *PLoS ONE* **2020**, *15*, e0237814. [[CrossRef](#)]
75. Zanello, S.; Watrin, F.; Mebarek, S.; Marly, F.; Roussel, M.; Gire, C.; Diene, G.; Tauber, M.; Muscatelli, F.; Hilaire, G. Necdin plays a role in the serotonergic modulation of the mouse respiratory network: Implication for Prader-Willi syndrome. *J. Neurosci.* **2008**, *28*, 1745–1755. [[CrossRef](#)]
76. Ren, J.; Lee, S.; Pagliardini, S.; Gérard, M.; Stewart, C.L.; Greer, J.J.; Wevrick, R. Absence of Ndn, encoding the Prader-Willi syndrome-deleted gene necdin, results in congenital deficiency of central respiratory drive in neonatal mice. *J. Neurosci.* **2003**, *23*, 1569–1573. [[CrossRef](#)]
77. Rieusset, A.; Schaller, F.; Unmehopa, U.; Matarazzo, V.; Watrin, F.; Linke, M.; Georges, B.; Bischof, J.; Dijkstra, F.; Bloemsma, M.; et al. Stochastic loss of silencing of the imprinted Ndn/NDN allele, in a mouse model and humans with prader-willi syndrome, has functional consequences. *PLoS Genet.* **2013**, *9*, e1003752. [[CrossRef](#)]
78. Matarazzo, V.; Caccialupi, L.; Schaller, F.; Shvarev, Y.; Kourdougli, N.; Bertoni, A.; Menuet, C.; Voituren, N.; Deneris, E.; Gaspar, P.; et al. Necdin shapes serotonergic development and SERT activity modulating breathing in a mouse model for Prader-Willi syndrome. *eLife* **2017**, *6*. [[CrossRef](#)] [[PubMed](#)]
79. Wu, R.N.; Hung, W.C.; Chen, C.T.; Tsai, L.P.; Lai, W.S.; Min, M.Y.; Wong, S.B. Firing activity of locus coeruleus noradrenergic neurons decreases in necdin-deficient mice, an animal model of Prader-Willi syndrome. *J. Neurodev. Disord.* **2020**, *12*, 21. [[CrossRef](#)]

80. Lu, R.; Dong, Y.; Li, J.D. Necdin regulates BMAL1 stability and circadian clock through SGT1-HSP90 chaperone machinery. *Nucleic Acids Res.* **2020**, *48*, 7944–7957. [[CrossRef](#)] [[PubMed](#)]
81. Chamberlain, S.J.; Johnstone, K.A.; DuBose, A.J.; Simon, T.A.; Bartolomei, M.S.; Resnick, J.L.; Brannan, C.I. Evidence for genetic modifiers of postnatal lethality in PWS-IC deletion mice. *Hum. Mol. Genet.* **2004**, *13*, 2971–2977. [[CrossRef](#)] [[PubMed](#)]
82. Relkovic, D.; Doe, C.M.; Humby, T.; Johnstone, K.A.; Resnick, J.L.; Holland, A.J.; Hagan, J.J.; Wilkinson, L.S.; Isles, A.R. Behavioural and cognitive abnormalities in an imprinting centre deletion mouse model for Prader–Willi syndrome. *Eur. J. Neurosci.* **2010**, *31*, 156–164. [[CrossRef](#)]
83. Doe, C.M.; Relkovic, D.; Garfield, A.S.; Dalley, J.W.; Theobald, D.E.; Humby, T.; Wilkinson, L.S.; Isles, A.R. Loss of the imprinted snoRNA mbii-52 leads to increased 5htr2c pre-RNA editing and altered 5HT2CR-mediated behaviour. *Hum. Mol. Genet.* **2009**, *18*, 2140–2148. [[CrossRef](#)] [[PubMed](#)]
84. Davies, J.R.; Humby, T.; Dwyer, D.M.; Garfield, A.S.; Furby, H.; Wilkinson, L.S.; Wells, T.; Isles, A.R. Calorie seeking, but not hedonic response, contributes to hyperphagia in a mouse model for Prader-Willi syndrome. *Eur. J. Neurosci.* **2015**, *42*, 2105–2113. [[CrossRef](#)]
85. Davies, J.R.; Wilkinson, L.S.; Isles, A.R.; Humby, T. Prader-Willi syndrome imprinting centre deletion mice have impaired baseline and 5-HT2CR-mediated response inhibition. *Hum. Mol. Genet.* **2019**, *28*, 3013–3023. [[CrossRef](#)]
86. Relkovic, D.; Humby, T.; Hagan, J.J.; Wilkinson, L.S.; Isles, A.R. Enhanced appetitive learning and reversal learning in a mouse model for Prader-Willi syndrome. *Behav. Neurosci.* **2012**, *126*, 488–492. [[CrossRef](#)]
87. Johnstone, K.A.; DuBose, A.J.; Futtner, C.R.; Elmore, M.D.; Brannan, C.I.; Resnick, J.L. A human imprinting centre demonstrates conserved acquisition but diverged maintenance of imprinting in a mouse model for Angelman syndrome imprinting defects. *Hum. Mol. Genet.* **2006**, *15*, 393–404. [[CrossRef](#)] [[PubMed](#)]
88. Pace, M.; Falappa, M.; Freschi, A.; Balzani, E.; Berteotti, C.; Lo Martire, V.; Kaveh, F.; Hovig, E.; Zoccoli, G.; Amici, R.; et al. Loss of Snord116 impacts lateral hypothalamus, sleep, and food-related behaviors. *JCI Insight* **2020**, *5*. [[CrossRef](#)] [[PubMed](#)]
89. Lassi, G.; Priano, L.; Maggi, S.; Garcia-Garcia, C.; Balzani, E.; El-Assawy, N.; Pagani, M.; Tinarelli, F.; Giardino, D.; Mauro, A.; et al. Deletion of the Snord116/SNORD116 Alters Sleep in Mice and Patients with Prader-Willi Syndrome. *Sleep* **2016**, *39*, 637–644. [[CrossRef](#)]
90. Adhikari, A.; Copping, N.A.; Onaga, B.; Pride, M.C.; Coulson, R.L.; Yang, M.; Yasui, D.H.; LaSalle, J.M.; Silverman, J.L. Cognitive deficits in the Snord116 deletion mouse model for Prader-Willi syndrome. *Neurobiol. Learn Mem.* **2019**, *165*, 106874. [[CrossRef](#)] [[PubMed](#)]
91. Poley-Wolf, J.; Lam, B.Y.; Larder, R.; Tadross, J.; Rimmington, D.; Bosch, F.; Cenzano, V.J.; Ayuso, E.; Ma, M.K.; Rainbow, K.; et al. Hypothalamic loss of Snord116 recapitulates the hyperphagia of Prader-Willi syndrome. *J. Clin. Investig.* **2018**, *128*, 960–969. [[CrossRef](#)]
92. Burnett, L.C.; Hubner, G.; LeDuc, C.A.; Morabito, M.V.; Carli, J.F.M.; Leibel, R.L. Loss of the imprinted, non-coding Snord116 gene cluster in the interval deleted in the Prader Willi syndrome results in murine neuronal and endocrine pancreatic developmental phenotypes. *Hum. Mol. Genet.* **2017**, *26*, 4606–4616. [[CrossRef](#)] [[PubMed](#)]
93. Burnett, L.C.; LeDuc, C.A.; Sulsona, C.R.; Paull, D.; Rausch, R.; Eddiry, S.; Carli, J.F.; Morabito, M.V.; Skowronski, A.A.; Hubner, G.; et al. Deficiency in prohormone convertase PC1 impairs prohormone processing in Prader-Willi syndrome. *J. Clin. Investig.* **2017**, *127*, 293–305. [[CrossRef](#)] [[PubMed](#)]
94. Powell, W.T.; Coulson, R.L.; Crary, F.K.; Wong, S.S.; Ach, R.A.; Tsang, P.; Alice Yamada, N.; Yasui, D.H.; LaSalle, J.M. A Prader-Willi locus lncRNA cloud modulates diurnal genes and energy expenditure. *Hum. Mol. Genet.* **2013**, *22*, 4318–4328. [[CrossRef](#)]
95. Qi, Y.; Purtell, L.; Fu, M.; Lee, N.J.; Aepler, J.; Zhang, L.; Loh, K.; Enriquez, R.F.; Baldock, P.A.; Zolotukhin, S.; et al. Snord116 is critical in the regulation of food intake and body weight. *Sci. Rep.* **2016**, *6*, 18614. [[CrossRef](#)] [[PubMed](#)]
96. Purtell, L.; Qi, Y.; Campbell, L.; Sainsbury, A.; Herzog, H. Adult-onset deletion of the Prader-Willi syndrome susceptibility gene Snord116 in mice results in reduced feeding and increased fat mass. *Transl. Pediatr.* **2017**, *6*, 88–97. [[CrossRef](#)]
97. Rozhdestvensky, T.S.; Robeck, T.; Galiveti, C.R.; Raabe, C.A.; Seeger, B.; Wolters, A.; Gubar, L.V.; Brosius, J.; Skryabin, B.V. Maternal transcription of non-protein coding RNAs from the PWS-critical region rescues growth retardation in mice. *Sci. Rep.* **2016**, *6*, 20398. [[CrossRef](#)] [[PubMed](#)]
98. Coulson, R.L.; Powell, W.T.; Yasui, D.H.; Dileep, G.; Resnick, J.; LaSalle, J.M. Prader-Willi locus Snord116 RNA processing requires an active endogenous allele and neuron-specific splicing by Rbfox3/NeuN. *Hum. Mol. Genet.* **2018**, *27*, 4051–4060. [[CrossRef](#)]
99. Wu, M.Y.; Jiang, M.; Zhai, X.; Beaudet, A.L.; Wu, R.C. An unexpected function of the Prader-Willi syndrome imprinting center in maternal imprinting in mice. *PLoS ONE* **2012**, *7*, e34348. [[CrossRef](#)]
100. Qi, Y.; Purtell, L.; Fu, M.; Zhang, L.; Zolotukhin, S.; Campbell, L.; Herzog, H. Hypothalamus Specific Re-Introduction of SNORD116 into Otherwise Snord116 Deficient Mice Increased Energy Expenditure. *J. Neuroendocrinol.* **2017**, *29*. [[CrossRef](#)]
101. Jonkers, J.; van Amerongen, R.; van der Valk, M.; Robanus-Maandag, E.; Molenaar, M.; Destrée, O.; Berns, A. In vivo analysis of Frat1 deficiency suggests compensatory activity of Frat3. *Mech. Dev.* **1999**, *88*, 183–194. [[CrossRef](#)]
102. Kobayashi, S.; Kohda, T.; Ichikawa, H.; Ogura, A.; Ohki, M.; Kaneko-Ishino, T.; Ishino, F. Paternal expression of a novel imprinted gene, Peg12/Frat3, in the mouse 7C region homologous to the Prader-Willi syndrome region. *Biochem. Biophys. Res. Commun.* **2002**, *290*, 403–408. [[CrossRef](#)]

103. Abreu, A.P.; Dauber, A.; Macedo, D.B.; Noel, S.D.; Brito, V.N.; Gill, J.C.; Cukier, P.; Thompson, I.R.; Navarro, V.M.; Gagliardi, P.C.; et al. Central Precocious Puberty Caused by Mutations in the Imprinted Gene MKRN3. *N. Engl. J. Med.* **2013**, *368*, 2467–2475. [[CrossRef](#)] [[PubMed](#)]
104. Kanber, D.; Giltay, J.; Wieczorek, D.; Zogel, C.; Hochstenbach, R.; Caliebe, A.; Kuechler, A.; Horsthemke, B.; Buiting, K. A paternal deletion of MKRN3, MAGEL2 and NDN does not result in Prader-Willi syndrome. *Eur. J. Hum. Genet.* **2009**, *17*, 582–590. [[CrossRef](#)] [[PubMed](#)]
105. Lee, S.; Walker, C.L.; Wevrick, R. Prader-Willi syndrome transcripts are expressed in phenotypically significant regions of the developing mouse brain. *Gene Expr. Patterns* **2003**, *3*, 599–609. [[CrossRef](#)]
106. Lee, S.; Kozlov, S.; Hernandez, L.; Chamberlain, S.J.; Brannan, C.I.; Stewart, C.L.; Wevrick, R. Expression and imprinting of MAGEL2 suggest a role in Prader-willi syndrome and the homologous murine imprinting phenotype. *Hum. Mol. Genet.* **2000**, *9*, 1813–1819. [[CrossRef](#)] [[PubMed](#)]
107. Hao, Y.H.; Doyle, J.M.; Ramanathan, S.; Gomez, T.S.; Jia, D.; Xu, M.; Chen, Z.J.; Billadeau, D.D.; Rosen, M.K.; Potts, P.R. Regulation of WASH-dependent actin polymerization and protein trafficking by ubiquitination. *Cell* **2013**, *152*, 1051–1064. [[CrossRef](#)] [[PubMed](#)]
108. Doyle, J.M.; Gao, J.; Wang, J.; Yang, M.; Potts, P.R. MAGE-RING protein complexes comprise a family of E3 ubiquitin ligases. *Mol. Cell* **2010**, *39*, 963–974. [[CrossRef](#)]
109. McCarthy, J.; Lupo, P.J.; Kovar, E.; Rech, M.; Bostwick, B.; Scott, D.; Kraft, K.; Roscioli, T.; Charrow, J.; Schrier Vergano, S.A.; et al. Schaaf-Yang syndrome overview: Report of 78 individuals. *Am. J. Med. Genet. Part A* **2018**, *176*, 2564–2574. [[CrossRef](#)]
110. Fountain, M.D.; Aten, E.; Cho, M.T.; Juusola, J.; Walkiewicz, M.A.; Ray, J.W.; Xia, F.; Yang, Y.; Graham, B.H.; Bacino, C.A.; et al. The phenotypic spectrum of Schaaf-Yang syndrome: 18 new affected individuals from 14 families. *Genet. Med.* **2017**, *19*, 45–52. [[CrossRef](#)]
111. Schaaf, C.P.; Gonzalez-Garay, M.L.; Xia, F.; Potocki, L.; Gripp, K.W.; Zhang, B.; Peters, B.A.; McElwain, M.A.; Drmanac, R.; Beaudet, A.L.; et al. Truncating mutations of MAGEL2 cause Prader-Willi phenotypes and autism. *Nat. Genet.* **2013**, *45*, 1405–1408. [[CrossRef](#)] [[PubMed](#)]
112. Tennesse, A.A.; Wevrick, R. Impaired Hypothalamic Regulation of Endocrine Function and Delayed Counterregulatory Response to Hypoglycemia in Magel2-Null Mice. *Endocrinology* **2011**, *152*, 967–978. [[CrossRef](#)]
113. Fountain, M.D.; Tao, H.; Chen, C.-A.; Yin, J.; Schaaf, C.P. Magel2 knockout mice manifest altered social phenotypes and a deficit in preference for social novelty. *Genes Brain Behav.* **2017**, *16*, 592–600. [[CrossRef](#)]
114. Kuwajima, T.; Hasegawa, K.; Yoshikawa, K. Necdin promotes tangential migration of neocortical interneurons from basal forebrain. *J. Neurosci.* **2010**, *30*, 3709–3714. [[CrossRef](#)] [[PubMed](#)]
115. Tennesse, A.A.; Gee, C.B.; Wevrick, R. Loss of the Prader-Willi syndrome protein necdin causes defective migration, axonal outgrowth, and survival of embryonic sympathetic neurons. *Dev. Dyn.* **2008**, *237*, 1935–1943. [[CrossRef](#)]
116. Gabriel, J.M.; Gray, T.A.; Stubbs, L.; Saitoh, S.; Ohta, T.; Nicholls, R.D. Structure and function correlations at the imprinted mouse Snrpn locus. *Mamm. Genome.* **1998**, *9*, 788–793. [[CrossRef](#)]
117. Chai, J.H.; Locke, D.P.; Ohta, T.; Greally, J.M.; Nicholls, R.D. Retrotransposed genes such as Frat3 in the mouse Chromosome 7C Prader-Willi syndrome region acquire the imprinted status of their insertion site. *Mamm. Genome* **2001**, *12*, 813–821. [[CrossRef](#)]
118. Brosius, J.; Tiedge, H. Reverse transcriptase: Mediator of genomic plasticity. *Virus Genes* **1995**, *11*, 163–179. [[CrossRef](#)] [[PubMed](#)]
119. Glenn, C.C.; Saitoh, S.; Jong, M.T.; Filbrandt, M.M.; Surti, U.; Driscoll, D.J.; Nicholls, R.D. Gene structure, DNA methylation, and imprinted expression of the human SNRPN gene. *Am. J. Hum. Genet.* **1996**, *58*, 335–346.
120. Gray, T.A.; Saitoh, S.; Nicholls, R.D. An imprinted, mammalian bicistronic transcript encodes two independent proteins. *Proc. Natl. Acad. Sci. USA* **1999**, *96*, 5616–5621. [[CrossRef](#)]
121. Li, H.; Zhao, P.; Xu, Q.; Shan, S.; Hu, C.; Qiu, Z.; Xu, X. The autism-related gene SNRPN regulates cortical and spine development via controlling nuclear receptor Nr4a1. *Sci. Rep.* **2016**, *6*, 1–10. [[CrossRef](#)] [[PubMed](#)]
122. Grimaldi, K.; Gerrelli, D.; Sharpe, N.G.; Lund, T.; Latchman, D.S. The intronless mouse gene for the tissue specific splicing protein SmN is a processed pseudogene containing a stop codon after thirty-one amino acids. *DNA Seq.* **1992**, *2*, 241–246. [[CrossRef](#)]
123. Lee, M.S.; Lin, Y.S.; Deng, Y.F.; Hsu, W.T.; Shen, C.C.; Cheng, Y.H.; Huang, Y.T.; Li, C. Modulation of alternative splicing by expression of small nuclear ribonucleoprotein polypeptide N. *FEBS J.* **2014**, *281*, 5194–5207. [[CrossRef](#)] [[PubMed](#)]
124. Bettio, D.; Rizzi, N.; Giardino, D.; Grugni, G.; Briscioli, V.; Selicorni, A.; Carnevale, F.; Larizza, L. FISH analysis in Prader-Willi and Angelman syndrome patients. *Am. J. Med. Genet.* **1995**, *56*, 224–228. [[CrossRef](#)]
125. Buiting, K.; Saitoh, S.; Gross, S.; Dittrich, B.; Schwartz, S.; Nicholls, R.D.; Horsthemke, B. Inherited microdeletions in the Angelman and Prader-Willi syndromes define an imprinting centre on human chromosome 15. *Nat. Genet.* **1995**, *9*, 395–400. [[CrossRef](#)]
126. Ohta, T.; Gray, T.A.; Rogan, P.K.; Buiting, K.; Gabriel, J.M.; Saitoh, S.; Muralidhar, B.; Bilienska, B.; Krajewska-Walasek, M.; Driscoll, D.J.; et al. Imprinting-mutation mechanisms in Prader-Willi syndrome. *Am. J. Hum. Genet.* **1999**, *64*, 397–413. [[CrossRef](#)] [[PubMed](#)]
127. Galiveti, C.R.; Raabe, C.A.; Konthur, Z.; Rozhdestvensky, T.S. Differential regulation of non-protein coding RNAs from Prader-Willi Syndrome locus. *Sci. Rep.* **2014**, *4*, 6445. [[CrossRef](#)]
128. Cavallé, J.; Buiting, K.; Kieffmann, M.; Lalande, M.; Brannan, C.I.; Horsthemke, B.; Bachelier, J.P.; Brosius, J.; Hüttenhofer, A. Identification of brain-specific and imprinted small nucleolar RNA genes exhibiting an unusual genomic organization. *Proc. Natl. Acad. Sci. USA* **2000**, *97*, 14311–14316. [[CrossRef](#)]

129. Cavaillé, J. Box C/D small nucleolar RNA genes and the Prader-Willi syndrome: A complex interplay. *Wiley Interdiscip. Rev. RNA* **2017**, *8*. [[CrossRef](#)] [[PubMed](#)]
130. Meguro, M.; Mitsuya, K.; Nomura, N.; Kohda, M.; Kashiwagi, A.; Nishigaki, R.; Yoshioka, H.; Nakao, M.; Oishi, M.; Oshimura, M. Large-scale evaluation of imprinting status in the Prader-Willi syndrome region: An imprinted direct repeat cluster resembling small nucleolar RNA genes. *Hum. Mol. Genet.* **2001**, *10*, 383–394. [[CrossRef](#)] [[PubMed](#)]
131. Ding, F.; Prints, Y.; Dhar, M.S.; Johnson, D.K.; Garnacho-Montero, C.; Nicholls, R.D.; Francke, U. Lack of Pwcr1/MBII-85 snoRNA is critical for neonatal lethality in Prader-Willi syndrome mouse models. *Mamm. Genome* **2005**, *16*, 424–431. [[CrossRef](#)]
132. Coulson, R.L.; Yasui, D.H.; Dunaway, K.W.; Laufer, B.I.; Vogel Ciernia, A.; Zhu, Y.; Mordaunt, C.E.; Totah, T.S.; LaSalle, J.M. Snord116-dependent diurnal rhythm of DNA methylation in mouse cortex. *Nat. Commun.* **2018**, *9*, 1616. [[CrossRef](#)]
133. Chagraoui, A.; Thibaut, F.; Skiba, M.; Thuillez, C.; Bourin, M. 5-HT_{2C} receptors in psychiatric disorders: A review. *Prog. Neuropsychopharmacol. Biol. Psychiatry* **2016**, *66*, 120–135. [[CrossRef](#)]
134. Palacios, J.M.; Pazos, A.; Hoyer, D. A short history of the 5-HT_{2C} receptor: From the choroid plexus to depression, obesity and addiction treatment. *Psychopharmacology* **2017**, *234*, 1395–1418. [[CrossRef](#)]
135. Morabito, M.V.; Ulbricht, R.J.; O’Neil, R.T.; Airey, D.C.; Lu, P.; Zhang, B.; Wang, L.; Emeson, R.B. High-throughput multiplexed transcript analysis yields enhanced resolution of 5-hydroxytryptamine 2C receptor mRNA editing profiles. *Mol. Pharmacol.* **2010**, *77*, 895–902. [[CrossRef](#)]
136. Werry, T.D.; Loiacono, R.; Sexton, P.M.; Christopoulos, A. RNA editing of the serotonin 5HT_{2C} receptor and its effects on cell signalling, pharmacology and brain function. *Pharmacol. Ther.* **2008**, *119*, 7–23. [[CrossRef](#)] [[PubMed](#)]
137. Kishore, S.; Stamm, S. The snoRNA HBII-52 regulates alternative splicing of the serotonin receptor 2C. *Science* **2006**, *311*, 230–232. [[CrossRef](#)] [[PubMed](#)]
138. Garfield, A.S.; Davies, J.R.; Burke, L.K.; Furby, H.V.; Wilkinson, L.S.; Heisler, L.K.; Isles, A.R. Increased alternate splicing of Htr2c in a mouse model for Prader-Willi syndrome leads disruption of 5HT_{2C} receptor mediated appetite. *Mol. Brain* **2016**, *9*, 95. [[CrossRef](#)]
139. Raabe, C.A.; Voss, R.; Kummerfeld, D.-M.; Brosius, J.; Galiveti, C.R.; Wolters, A.; Seggewiss, J.; Huge, A.; Skryabin, B.V.; Rozhdestvensky, T.S. Ectopic expression of Snord115 in choroid plexus interferes with editing but not splicing of 5-Ht2c receptor pre-mRNA in mice. *Sci. Rep.* **2019**, *9*, 4300. [[CrossRef](#)] [[PubMed](#)]
140. Bochukova, E.G.; Lawler, K.; Croizier, S.; Keogh, J.M.; Patel, N.; Strohbehn, G.; Lo, K.K.; Humphrey, J.; Hokken-Koelega, A.; Damen, L.; et al. A Transcriptomic Signature of the Hypothalamic Response to Fasting and BDNF Deficiency in Prader-Willi Syndrome. *Cell Rep.* **2018**, *22*, 3401–3408. [[CrossRef](#)]
141. Vitali, P.; Basyuk, E.; Le Meur, E.; Bertrand, E.; Muscatelli, F.; Cavaillé, J.; Huttenhofer, A. ADAR2-mediated editing of RNA substrates in the nucleolus is inhibited by C/D small nucleolar RNAs. *J. Cell Biol.* **2005**, *169*, 745–753. [[CrossRef](#)]
142. Nakatani, J.; Tamada, K.; Hatanaka, F.; Ise, S.; Ohta, H.; Inoue, K.; Tomonaga, S.; Watanabe, Y.; Chung, Y.J.; Banerjee, R.; et al. Abnormal behavior in a chromosome-engineered mouse model for human 15q11-13 duplication seen in autism. *Cell* **2009**, *137*, 1235–1246. [[CrossRef](#)]
143. Mo, D.; Raabe, C.A.; Reinhardt, R.; Brosius, J.; Rozhdestvensky, T.S. Alternative processing as evolutionary mechanism for the origin of novel nonprotein coding RNAs. *Genome Biol. Evol.* **2013**, *5*, 2061–2071. [[CrossRef](#)]
144. Brosius, J. The fragmented gene. *Ann. N. Y. Acad. Sci.* **2009**, *1178*, 186–193. [[CrossRef](#)]
145. Zhang, Q.; Bouma, G.J.; McClellan, K.; Tobet, S. Hypothalamic expression of snoRNA Snord116 is consistent with a link to the hyperphagia and obesity symptoms of Prader-Willi syndrome. *Int. J. Dev. Neurosci.* **2012**, *30*, 479–485. [[CrossRef](#)]
146. Castle, J.C.; Armour, C.D.; Lower, M.; Haynor, D.; Biery, M.; Bouzek, H.; Chen, R.; Jackson, S.; Johnson, J.M.; Rohl, C.A.; et al. Digital genome-wide ncRNA expression, including SnoRNAs, across 11 human tissues using polyA-neutral amplification. *PLoS ONE* **2010**, *5*, e11779. [[CrossRef](#)]
147. Skryabin, B.V.; Kummerfeld, D.M.; Gubar, L.; Seeger, B.; Kaiser, H.; Stegemann, A.; Roth, J.; Meuth, S.G.; Pavenstadt, H.; Sherwood, J.; et al. Pervasive head-to-tail insertions of DNA templates mask desired CRISPR-Cas9-mediated genome editing events. *Sci. Adv.* **2020**, *6*, eaax2941. [[CrossRef](#)]
148. Smirnov, A.; Fishman, V.; Yunusova, A.; Korablev, A.; Serova, I.; Skryabin, B.V.; Rozhdestvensky, T.S.; Battulin, N. DNA barcoding reveals that injected transgenes are predominantly processed by homologous recombination in mouse zygote. *Nucleic. Acids Res.* **2020**, *48*, 719–735. [[CrossRef](#)] [[PubMed](#)]
149. Sibilias, M.; Wagner, E.F. Strain-dependent epithelial defects in mice lacking the EGF receptor. *Science* **1995**, *269*, 234–238. [[CrossRef](#)] [[PubMed](#)]
150. Carias, K.V.; Wevrick, R. Preclinical Testing in Translational Animal Models of Prader-Willi Syndrome: Overview and Gap Analysis. *Mol. Ther. Methods Clin. Dev.* **2019**, *13*, 344–358. [[CrossRef](#)] [[PubMed](#)]
151. Good, D.J.; Kocher, M.A. Phylogenetic Analysis of the SNORD116 Locus. *Genes* **2017**, *8*, 358. [[CrossRef](#)]